IOP Publishing New J. Phys. 27 (2025) 074603 https://doi.org/10.1088/1367-2630/adee40

New Journal of Physics
The open access journal at the forefront of physics

Deutsche Physikalische Gesellschaft DPG
IOP Institute of Physics

Published in partnership with: Deutsche Physikalische Gesellschaft and the Institute of Physics

CrossMark

OPEN ACCESS

RECEIVED
20 February 2025

REVISED
30 June 2025

ACCEPTED FOR PUBLICATION
10 July 2025

PUBLISHED
24 July 2025

PAPER

Series representation approach to stochastic processes with complete and incomplete renewal resetting

Kacper Taźbierski[1], **Ralf Metzler**[2,3,*] and **Marcin Magdziarz**[1]

[1] Faculty of Pure and Applied Mathematics, Hugo Steinhaus Centre, Wroclaw University of Science and Technology, Wyspianskiego 27, 50-370 Wroclaw, Poland
[2] Institute of Physics & Astronomy, University of Potsdam, 14476 Potsdam-Golm, Germany
[3] Asia Pacific Centre for Theoretical Physics, Pohang 37673, Republic of Korea
[*] Author to whom any correspondence should be addressed.

E-mail: rmetzler@uni-potsdam.de, kacper.tazbierski@pwr.edu.pl and marcin.magdziarz@pwr.edu.pl

Keywords: diffusion, resetting, first passage times

Abstract
We introduce a series representation for stochastic processes in which resetting is driven by a renewal process. Both memory-erasing ('complete') resetting and simple position shifting ('incomplete resetting') are considered. Our approach allows us to calculate the previously unknown joint two-time probability density function and the autocorrelation function in a straightforward manner. We also study the associated first-passage problem, reporting general results for the case of complete resetting. In each case we inspect the scenarios of exponentially (Poissonian resetting) and mixture-exponentially distributed inter-resetting times, with Brownian motion and scaled Brownian motion as the parental processes. We also utilise the results obtained for the mixture-exponential inter-resetting times as an approximation for more general classes of distributions.

1. Introduction

In one of the most cited papers in the theory of stochastic processes, Smoluchowski derived the diffusion limit for chemical reactions of two molecules in 1916 [1, 2]. However, even before him the problem of 'first-passage' of a stochastic process was anticipated by Bachelier in the context of his 1900 thesis of financial markets [3], and Lundberg considered such concepts in insurance mathematics in 1903 [4]. Schrödinger formulated an integral equation approach to first-passage in 1915 [5]. Today, the problem of first-passage has widespread applications in physics, chemistry, biology, ecology, economics, and beyond [6–8]. We note that from a mathematical point of view, the first-passage problem is related to the theories on the gambler's ruin started by Bernoulli, de Moivre, Lagrange, and Laplace [9, 10].

In typical settings in infinite systems, the probability density function (PDF) of first-passage times (FPT) has power-law tails such that the mean first-passage time (MFPT) diverges [6, 7]. The MFPT or its global variant is finite in bounded geometries [11, 12], however, the actual FPTs can be defocused over several orders of magnitude [13–15]. In both cases, short FPTs correspond to 'direct' trajectories, moving more or less straight from the initial location to the target [13–15]. Conversely, long FPTs are caused by long(er) excursions away from the target, during which the diffusing particle forgets its initial point of release.

A by-now highly prominent mechanism to enforce finite MFPTs and a stationary PDF (the 'non-equilibrium steady state' (NESS)) even in infinite domains is 'stochastic resetting' (SR) [16–19]. In its simplest version, SR considers a particle performing a Brownian motion, that is interrupted by repeated restarts, resetting the particle to its starting position; this can occur at fixed periods in time or stochastically, with a fixed rate [16–18, 20–22]. In such an SR scenario the MFPT to a certain distance from its starting point can be minimised for a specific resetting frequency [16–18, 20]. This minimum represents a tradeoff between the fact that SR avoids long departures away from the target while too frequent SR events do not allow the particle to move sufficiently far to actually reach the target [16–18, 20].

It has been shown that quite generic statements can be made concerning the SR-rate for minimal MFPTs, the coefficient of variation of FPT fluctuations, and extremes of SR [23–25]. It was shown that SR can be phrased as a renewal process [26], and the linear response behaviour and fluctuation-dissipation relations for SR were established [26, 27]. Recently, the concept was also extended to quantum systems [28, 29]. Applications of SR have been discussed, inter alia, in the modelling of animal foraging [30], population dynamics in the case of sudden population catastrophes [31], stochastic optimisation in computational sampling [18, 32, 33], ecology [34] or enzymatic reactions [35], see also [18]. SR also found applications in reaction-diffusion systems, see, for instance, reference [36], in which binary models of aggregation with constant kernel are subjected to SR; or reference [37], in which the statistical mechanics of the coagulation-diffusion process with SR are studied. In particular, the effect of SR was demonstrated experimentally directly in different settings [20, 38–40].

SR models with both Markovian and non-Markovian resetting have been studied in literature. Resetting guided by a Poisson process, with possible inhomogeneity in space or time, has been extensively studied [18]. We previously considered Brownian motion undergoing incomplete resetting, for which the process guiding the resetting was an inhomogeneous Poisson process rather than a renewal process [41]. In some cases SR was considered on a countable subset of the time domain for which a geometric distribution was used to maintain Markovianity [42]. Inhomogeneity was considered in both time and space [18, 41]. Non-Markovian systems were considered using a renewal process guiding the resetting in, e.g. [43]. Scaled Brownian Motion (SBM) was considered with complete [44] as well as incomplete resetting [45]—note that the second case was called 'non-renewal resetting', as the process does not lose its memory after the resetting event, but the underlying mechanism rests on a renewal process. Incomplete resetting models are processes that randomly shift to the origin, but their dynamics is influenced by temporally inhomogeneous media: imagine a resetting particle in an environment with time-varying temperature or a redenomination process, changing the face value of banknotes and coins in circulation, when the inflation rate is growing. This kind of process was also studies in the context of so-called velocity resetting [46].

SR in fractional Brownian motion and heterogeneous diffusion were analysed [47, 48] along with the associated ergodic properties. Continuous time random walks with SR and related ergodic properties were studied [49, 50]. Geometric Brownian motion with SR was analysed in [51, 52] and studied in the context of income inequality and mobility [53]. Heavy-tailed processes under complete Poissonian resetting were investigated [54] and shown to assume a Linnik distribution in the NESS [55]. Diffusion with SR on lattices and graphs and the associated MFPT were analysed in [56, 57], and SR in an electromagnetic field was considered in [58]. In [59] resetting of rotational diffusion was used in the description of polar molecules. [60] considered the interplay between noise induced stability and SR. Cost functions for SR were also studied [61]. Finally, the search for multiple targets by a diffusing particle with SR was studied [62]. Finally we mention the analysis of two competing searchers under subsystem restarts [63].

The De Vylder approximation is a method often used in financial or actuarial science and risk theory to approximate the distribution of aggregate claims in an insurance portfolio [64]. This technique simplifies complex distribution problems by fitting a mixture of exponential distributions to match the mean, variance, and skewness of the original distribution. It is particularly useful for providing quick and reasonably accurate estimates in situations in which exact calculations are infeasible due to the intricacy of the underlying models. This technique is also viable for a variety of uses in other disciplines, and we will employ it in the subsequent analysis in order to approximate certain parameters of resetting processes with complicated waiting-time distributions.

In the following we consider a new, alternative stochastic representation of the renewal resetting process, incorporating and generalising many previously obtained results for large classes of processes in a new framework, such as the autocorrelation function of Brownian motion and scaled Brownian motion undergoing Poissonian resetting, see [65]. The main advantages of the approach presented here are: the straightforward interpretability of the definitions and the possibility to use classical probability theory to obtain new results. In particular, using our framework we will obtain two-point distributions of the process under complete resetting and subsequently calculate the corresponding autocorrelation function. We will also utilise the mixture-exponential distributions to derive approximate results for more general classes of distributions. Already known results will be verified. Combining analytical and numerical tools we will check the effects of different types of resetting on the underlying system, in particular, the scenarios of complete and incomplete resetting. Among the properties of interest are the NESS, two-dimensional distributions, autocorrelations, and FPTs. The discussion covers a wide class of stopping times, for which only certain local properties of the process are measured.

The paper is organised as follows. We introduce our series representation approach in section 2. In section 3 we consider the PDFs and associated moments under resetting. First-passage problems will then be addressed in section 4, where we also derive a new MFPT approximation tool based on mixture-exponential distributions. We draw our conclusions in section 5.

2. Series representation of stochastic processes under resetting

In this section we introduce the series representation of stochastic processes under SR guided by a renewal process. Furthermore, we discuss the intuition behind the definition and visualise necessary concepts.

To this end, let us consider a sequence $\{X_j\}, j \in \mathbb{N}$, of identically distributed (IID) copies of a stochastic process $X(t)$ and an independent renewal process $N(t)$. We define the process under *complete SR* in terms of the series representation in the following way,

$$X_C(t) = \sum_{i=0}^{\infty} X_i(t-\tau_i)\,\mathbf{1}_{N(t)=i}, \quad x_r = X_C(0) = 0. \tag{1}$$

Moreover, we denote by τ_i the time instant of the ith resetting event, with $\tau_0 = 0$. Recall that the renewal process is a counting process in which the interarrival times are independent and IID random variables. A typical example of a renewal process is the standard Poisson process for which the interarrival times are IID exponentially distributed random variables. We can then write that $N(t) = \max\{i \in \mathbb{N} \,|\, \tau_i \leqslant t\}$. Note that since the $X_i(t)$ are IID, after each resetting event the memory of the process is completely lost. More precisely, the definition (1) is based on a sequence of IID processes $(X_i(t))$ with the same law as the original process $X(t)$. On each interval $[\tau_i, \tau_{i+1})$ the process takes the form

$$X_C(t)|(t \in [\tau_i, \tau_{i+1})) = X_i(t-\tau_i)|(t \in [\tau_i, \tau_{i+1})), \tag{2}$$

where we use the notation $A|B$ as A conditioned on B. This process behaves as the original process restarted anew at its origin, see figure 1. Putting together the successive inter-resetting intervals yields the final form (1).

For the case of *incomplete resetting*, the series representation of the resetting process assumes the form

$$X_P(t) = X(t) - \sum_{i=1}^{\infty} X(\tau_i)\,\mathbf{1}_{N(t)=i}. \tag{3}$$

Here the process is simply shifted during a resetting event by the value of the process at $t = \tau_i$. Note that in this case $X(t)$ is *not* replaced by its IID copy after the resetting event, as it was the case in (1), see the illustration in figure 2. When X has independent and stationary increments, the processes X_C and X_P are equivalent and both definitions (1) and (3) are interchangeable.

In the above, for simplicity we chose the resetting position $x_{\mathrm{r}} = 0$, any other case $x_{\mathrm{r}} \neq 0$ can be simplified via the shift $X' = X - x_{\mathrm{r}}$—we emphasise the importance of this transformation. The condition $x_{\mathrm{r}} = 0$ is also given through the assumption that the system is already in the resetting phase, albeit not necessarily in its stationary form. This assumption is relevant for processes such as geometric Brownian motion which can take only strictly positive values. In the case of incomplete resetting the situation is different. Namely, for models with inherent temporal or spatial inhomogeneities the properties of the processes will be significantly altered by this SR strategy. Looking again at geometric Brownian motion, we can see that incomplete resetting may allow the process to reach negative values even with a positive resetting point—which is not possible in the original process.

We recall another useful representation of a SR process. Assume that the underlying process $X(t)$ is given in terms of the stochastic differential Equation [66]

$$\mathrm{d}X(t) = \mu(t, X(t))\,\mathrm{d}t + \sigma(t, X(t))\,\mathrm{d}\xi(t), \quad X(0) = x_0 \tag{4}$$

with the driving noise $\xi(t)$ and the drift and diffusion parameters μ and σ. Now the process with incomplete resetting can be defined as [41]

$$\mathrm{d}X_P(t) = \mu(t, X_P(t))\,\mathrm{d}t + \sigma(t, X_P(t))\,\mathrm{d}\xi(t) + (x_r - X_P(t))\,\mathrm{d}N(t). \tag{5}$$

Here the resetting mechanism is introduced by the term $(x_r - X_P(t))\mathrm{d}N(t)$. In this formalism the simple case of Brownian motion under resetting can be introduced as

$$\mathrm{d}X_P(t) = \mathrm{d}B(t) + (x_r - X_P(t))\,\mathrm{d}N(t), \tag{6}$$

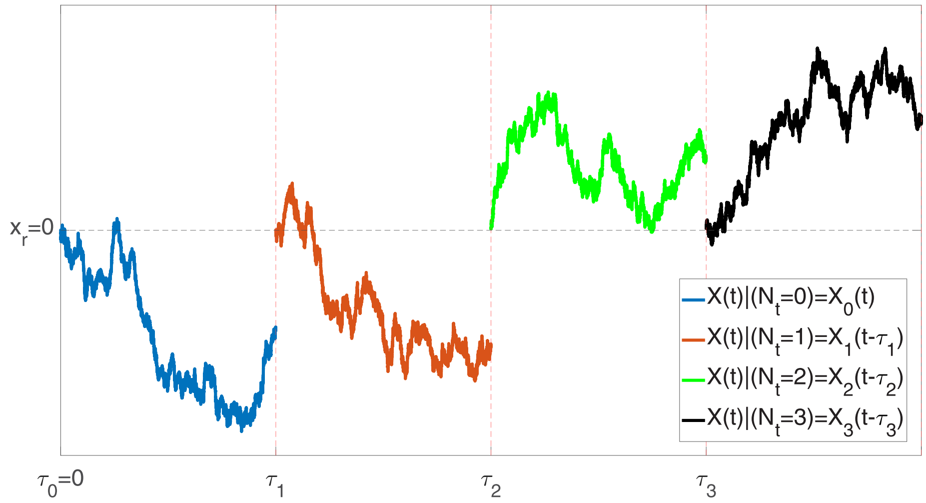

Figure 1. Visualisation of the definition of the series representation of SR. Here, we chose constant inter-resetting intervals for clarity.

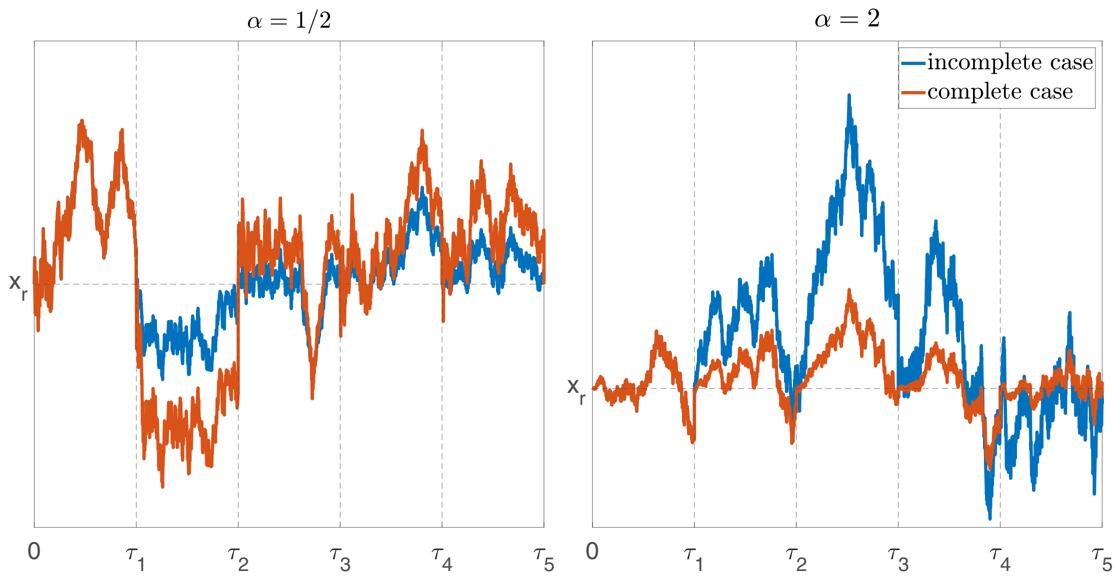

Figure 2. Comparison of the behaviour of SBM with complete and incomplete resetting in the subdiffusive (left panel, $\alpha < 1$) and superdiffusive (right panel, $\alpha > 1$) regimes. We used the same Gaussian increments for the simulations to underline the differences, thus on the first inter-resetting interval the processes are equal. In the subdiffusive regime we can see that the process with complete resetting achieves higher volatilities, while in the superdiffusive it is reversed, as expected.

where $B(t)$ represents Brownian motion. This approach can also be used to define complete resetting in a similar, but slightly more complicated manner,

$$\begin{aligned} \mathrm{d}X_C(t) = & \sum_{i=0}^{\infty} \left[\mathbf{1}_{N(t)=i} \left(\mu\left(t-\tau_i, X_C(t)\right)\mathrm{d}t + \sigma\left(t-\tau_i, X_C(t)\right)\mathrm{d}\xi_i\left(t-\tau_i\right)\right)\right] \\ & + \left(x_r - X_C(t)\right)\mathrm{d}N(t). \end{aligned} \tag{7}$$

Here we used a sequence of independent copies $\xi_i(t)$ of the noise process. The main difference between formulations (7) and (5) can be seen in the noise term. The single driving noise $\xi(t)$ in equation (5) is replaced by a sequence of IID noises $\xi_i(t)$ to reflect the memory loss of the driving force at each reset. The particular case of SBM[4] under incomplete resetting takes the form

$$\mathrm{d}X_C(t) = \sqrt{\alpha}\sum_{i=0}^{\infty}\mathbf{1}_{N(t)=i}(t-\tau_i)^{(\alpha-1)/2}\,\mathrm{d}B_i(t) + (x_r - X_C(t))\,\mathrm{d}N(t). \tag{8}$$

Here $B_i(t)$ are IID copies of Brownian motion $B(t)$. We used the fact that $B(t)$ has independent and stationary increments, allowing us to use the identity $\mathrm{d}B_i(t-\tau_i) \overset{D}{=} \mathrm{d}B_i(t)$[5]. For other examples of this approach see [41].

3. Characterisation of the resetting process by distributions and moments

In this section we calculate the PDF of stochastic process under SR in the complete and incomplete cases using the series representation introduce above. Moreover, we derive the two-dimensional distribution for complete resetting and obtain the autocorrelation function. We check the results by comparing to known cases as well as derive new results for SBM and mixed exponentially distributed inter-resetting times.

3.1. Distributions for complete resetting

3.1.1. PDF

For our calculations we use the law of total probability for the PDF p_{X_C} of the process $X_C(t)$, splitting the sample space according to the possible values of $N(t)$. Using the definition (1) of X_C we start with calculating the conditional distribution of $X_C(t)$ given that $N(t)=n$,

$$X_C(t)\,|\,(N(t)=n) = \sum_{i=0}^{\infty} X_i(t-\tau_i)\,\mathbf{1}_{N(t)=i}|\,(N(t)=n) = X_n(t-\tau_n)\,|\,(N(t)=n). \tag{9}$$

Here, we applied the independence of X_i and $N(t)$. The symbol $\mathbf{1}_A$ is the indicator of the set A (i.e. $\mathbf{1}_A = \mathbf{1}_A(x) = 1$ if $x\in A$ and $\mathbf{1}_A(x) = 0$ if $x \notin A$). These definitions lead us to

$$p_{X_C}(x,t)\,\mathrm{d}x = \mathbb{P}(X_C(t)\in(x,x+\mathrm{d}x)) = \sum_{n=0}^{\infty}\mathbb{P}(X_C(t)\in(x,x+\mathrm{d}x), N(t)=n), \tag{10}$$

where we used the law of total probability with respect to $N(t)$ outcomes. Now, using equation (9) we obtain

$$p_{X_C}(x,t)\,\mathrm{d}x = \sum_{n=0}^{\infty}\mathbb{P}(X_n(t-\tau_n)\in(x,x+\mathrm{d}x), N(t)=n). \tag{11}$$

We can rewrite the event $N(t)=n$ as $0\leqslant t-\tau_n < \Delta\tau_{n+1}$, with $\Delta\tau_{n+1} = \tau_{n+1}-\tau_n$. We then average over all possible τ_n outcomes using the law of total probability again,

$$p_{X_C}(x,t)\,\mathrm{d}x = \sum_{n=0}^{\infty}\int_0^t \mathbb{P}(X_n(t-u)\in(x,x+\mathrm{d}x), 0\leqslant t-u<\Delta\tau_{n+1})\,p_{\tau_n}(u)\,\mathrm{d}u. \tag{12}$$

Notice that the random variable $\Delta\tau_{n+1}$ is independent from X_n, resulting in

$$\begin{aligned} p_{X_C}(x,t)\,\mathrm{d}x &= \sum_{n=0}^{\infty}\int_0^t p_X(x,t-u)\,S_{\Delta\tau}(t-u)\,p_{\tau_n}(u)\,\mathrm{d}u\mathrm{d}x \\ &= p_X(x,t)\,S_{\Delta\tau}(t)\overset{t}{*}\sum_{n=0}^{\infty}p_{\tau_n}(t)\,\mathrm{d}x, \end{aligned} \tag{13}$$

where we denoted $f\overset{t}{*}g = \int_0^t f(t-u)g(u)\mathrm{d}u$ as a convolution with respect to the variable in the superscript, $S_X(x) = \mathbb{P}(X>x)$ as the survival probability of the random variable X, and used the renewal property, according to which

$$\Delta\tau \overset{D}{=} \Delta\tau_{n+1} = \tau_{n+1}-\tau_n \perp\!\!\!\perp \tau_n. \tag{14}$$

[4] SBM is a Gaussian process with correlator $\langle B_\alpha(s)B_\alpha(t)\rangle = \min\{s^\alpha, t^\alpha\}$, following the Langevin equation $\dot{x}(t) = \sqrt{2K(t)}\xi(t)$ with $K(t)\propto t^{\alpha-1}$ and the zero-mean white Gaussian noise $\xi(t)$ [67, 68].

[5] Here and in the following $\overset{D}{=}$ means 'equal in distribution'.

Here $\perp\!\!\!\perp$ stands for the statistical independence. In the classical case of Brownian motion under resetting, $p_X(x,t)$ would be the Gaussian propagator. Now we utilise the Laplace transformation

$$\mathscr{L}_t\{f(t)\}(s) = \int_0^\infty \mathrm{e}^{-st} f(t)\,\mathrm{d}t = \tilde{f}(s) \tag{15}$$

for further calculations. In particular, we will make extensive use of the convolution theorem

$$\mathscr{L}_t\{f(t) * g(t)\}(s) = \tilde{f}(s)\tilde{g}(s), \tag{16}$$

where the convolution operator $*$ is defined as $f(t) * g(t) = \int_0^t f(t')g(t-t')\mathrm{d}t'$.

Denoting the resetting intensity as $r(t) = \sum_{n=0}^\infty p_{\tau_n}(t)$, we obtain in Laplace space that

$$\tilde{r}(s) = \mathscr{L}_t\left\{\sum_{n=0}^\infty p_{\tau_n}(t)\right\}(s) = \sum_{n=0}^\infty \mathscr{L}_t\left\{p_{\Delta\tau}^{(*n)}(t)\right\}(s) = \sum_{n=0}^\infty \tilde{p}_{\Delta\tau}^n(s) = \frac{1}{1-\tilde{p}_{\Delta\tau}(s)} \tag{17}$$

for $s > 0$. Here $f^{(*n)}$ is the n-fold convolution of f with itself. When $N(t)$ is a Poisson process this simplifies to $r(t) = \delta(t) + r$, a sum of a Dirac-δ and a constant r, which correspond to the fact that the process starts at $t = 0$ and that the intensity of $N(t)$ is equal to r. The PDF of the process $X_C(t)$ thus takes on the form

$$p_{X_C}(x,t) = r(t) \overset{t}{*} S_{\Delta\tau}(t)\, p_X(x,t), \tag{18}$$

with the Laplace image

$$p_{X_C}(x,s) = \frac{\mathscr{L}_t\{p_X(x,t)\,S_{\Delta\tau}(t)\}(x,s)}{1-p_{\Delta\tau}(s)}. \tag{19}$$

Any space-average of the process of the form $\langle f(X_C(t))\rangle$ can then be easily obtained using equation (18), namely,

$$\langle f(X_C(t))\rangle = r(t) \overset{t}{*} S_{\Delta\tau}(t)\,\langle f(X(t))\rangle, \tag{20}$$

while for an appropriately smooth monotonic function f the distribution of $f(X_C(t))$ has the form

$$p_{f(X_C)}(x,t) = \frac{r(t) \overset{t}{*} S_{\Delta\tau}(t)\, p_X\left(f^{-1}(x), t\right)}{|f'(x)|}. \tag{21}$$

3.1.2. Two-dimensional PDF

We now focus on the important case of the joint two-time probability of the process at times t_1 and t_2, with $t_2 \geqslant t_1$. Again splitting the sample space according to all possible $(N(t_1), N(t_2))$ outcomes $(n, n+k)$, where $n, k \in \mathbb{N}$, we obtain

$$\begin{aligned}(X_C(t_1), X_C(t_2))\,\big|\,(N(t_1), N(t_2) = (n, n+k))\\ = (X_n(t_1-\tau_n), X_{n+k}(t_2-\tau_{n+k}))\,\big|\,(N(t_1), N(t_2) = (n, n+k)).\end{aligned} \tag{22}$$

The PDF of the process X_C at the two time points t_1, t_2 can now be calculated as

$$\begin{aligned}p_{X_C}(x_1, x_2, t_1, t_2)\,\mathrm{d}x_1\mathrm{d}x_2 &= \mathbb{P}(X_C(t_1) \in (x_1, x+\mathrm{d}x_1), X_C(t_2) \in (x_2, x_2+\mathrm{d}x_2))\\ &= \sum_{n,k=0}^\infty \mathbb{P}\big(X_n(t_1-\tau_n) \in (x_1, x+\mathrm{d}x_1), X_{n+k}(t_2-\tau_{n+k}) \in (x_2, x_2+\mathrm{d}x_2),\\ &\qquad N(t_1) = n, N(t_2) = n+k\big).\end{aligned} \tag{23}$$

For the special case $k = 0$, equation (23) simplifies to

$$\begin{aligned}&\sum_{n=0}^\infty \mathbb{P}\big(X_n(t_1-\tau_n) \in (x_1, x_1+\mathrm{d}x_1), X_n(t_2-\tau_n) \in (x_2, x_2+\mathrm{d}x_2),\\ &\qquad 0 \leqslant t_1-\tau_n \leqslant t_2-\tau_n < \Delta\tau_{n+1}\big),\end{aligned} \tag{24}$$

where we used the fact, that the events $\{N(t_1) = n, N(t_2) = n+k\}$, and $\{0 \leqslant t_1 - \tau_n \leqslant t_2 - \tau_n < \Delta\tau_{n+1}\}$ are equivalent. Now, let us use the law of total probability with respect to all the possible τ_n outcomes to get

$$\sum_{n=0}^{\infty}\int_0^{t_1}\mathbb{P}\big(X_n(t_1-u)\in(x_1,x_1+\mathrm{d}x_1),X_n(t_2-u)\in(x_2,x_2+\mathrm{d}x_2),$$
$$0\leqslant t_1-u\leqslant t_2-u<\Delta\tau_{n+1}\big)p_{\tau_n}(u)\mathrm{d}u$$
$$=\int_0^{t_1}p_X(x_1,x_2,t_1-u,t_2-u)\,S_{\Delta\tau}(t_2-u)\,r(u)\,\mathrm{d}u\mathrm{d}x_1\mathrm{d}x_2, \tag{25}$$

where we interchanged the summation and integration and used definition (17) for $r(t)$. Now for $k>0$ we know that

$$\{(N(t_1),N(t_2))=(n,n+k)\}=\{\tau_n\leqslant t_1<\tau_{n+1}\leqslant\tau_{n+k}\leq t_2<\tau_{n+k+1}\}. \tag{26}$$

For the renewal times we also have

$$\tau_{n+1}=\tau_n+\Delta\tau_{n+1},$$
$$\tau_{n+k}=\tau_n+\Delta\tau_{n+1}+\sum_{j=2}^{k}\Delta\tau_{n+j},$$
$$\tau_{n+k+1}=\tau_n+\Delta\tau_{n+1}+\sum_{j=2}^{k}\Delta\tau_{n+j}+\Delta\tau_{n+k+1}, \tag{27}$$

where $\sum_{j=2}^{k}\Delta\tau_{n+k}\stackrel{D}{=}\tau_{k-1}$. Using the above and conditioning on independent random variables $\tau_n,\Delta\tau_{n+1},\sum_{j=2}^{k}\Delta\tau_{n+k},\Delta\tau_{n+k+1}$, we get for the terms under the sum (23) that

$$\mathbb{P}\big(X_n(t_1-\tau_n)\in(x_1,x+\mathrm{d}x_1),X_{n+k}(t_2-\tau_{n+k})\in(x_2,x_2+\mathrm{d}x_2),$$
$$N(t_1)=n,N(t_2)=n+k\big)$$
$$=\int_0^{t_1}\mathrm{d}u\int_{t_1-u}^{t_2-u}\mathrm{d}w\int_0^{t_2-u-w}\mathrm{d}z\int_{t_2-u-w-z}^{\infty}\mathrm{d}y\,p_{\tau_n}(u)\,p_{\Delta\tau}(w)\,p_{\tau_{k-1}}(z)$$
$$\times\, p_{\Delta\tau}(y)\,p_X(x_1,t_1-u)\,p_X(x_2,t_2-u-w-z)\,\mathrm{d}x_1\mathrm{d}x_2, \tag{28}$$

where the one-dimensional PDF replaces the two-dimensional PDF due to the independence of the processes X_i,X_j for $i\neq j$. Now we can evaluate the sum (23). Note that the only n-dependent term is $p_{\tau_n}(u)$, summing up to $r(u)$. Moreover the only k-dependent term is $p_{\tau_{k-1}}(z)$, summing up to $r(z)$. The terms $k>0$ in equation (23) are now equal to

$$\sum_{n=0}^{\infty}\sum_{k=1}^{\infty}\int_0^{t_1}\mathrm{d}u\int_{t_1-u}^{t_2-u}\mathrm{d}w\int_0^{t_2-u-w}\mathrm{d}z\int_{t_2-u-w-z}^{\infty}\mathrm{d}y\,p_{\tau_n}(u)\,p_{\Delta\tau}(w)\,p_{\tau_{k-1}}(z)$$
$$\times\, p_{\Delta\tau}(y)\,p_X(x_1,t_1-u)\,p_X(x_2,t_2-u-w-z)\,\mathrm{d}x_1\mathrm{d}x_2$$
$$=\int_0^{t_1}r(u)\,p_X(x_1,t_1-u)\int_{t_1-u}^{t_2-u}p_{\Delta\tau}(w)\int_0^{t_2-u-w}r(z)$$
$$\times\, p_X(x_2,t_2-u-w-z)\times S_{\Delta\tau}(t_2-u-w-z)\,\mathrm{d}z\mathrm{d}w\mathrm{d}u\mathrm{d}x_1\mathrm{d}x_2. \tag{29}$$

Putting together the results (25) for $k=0$ and (29) for $k>0$ we obtain the final result

$$p_{X_C}(x_1,x_2,t_1,t_2)=\int_0^{t_1} p_X(x_1,x_2,t_1-u,t_2-u)\,S_{\Delta\tau}(t_2-u)\,r(u)\,\mathrm{d}u + \int_0^{t_1} r(u)\,p_X(x_1,t_1-u)\int_{t_1-u}^{t_2-u} p_{\Delta\tau}(w)\int_0^{t_2-u-w} r(z) \times p_X(x_2,t_2-u-w-z)\times S_{\Delta\tau}(t_2-u-w-z)\,\mathrm{d}z\mathrm{d}w\mathrm{d}u. \tag{30}$$

3.1.3. Autocorrelation

The autocorrelation $c_C(t_1,t_2)=\langle X_C(t_1)X_C(t_2)\rangle$ of the process under complete resetting can now be obtained from expression (30), via multiplying $p_{X_C}(x_1,x_2,t_1,t_2)$ by x_1x_2 and integrating

$$\begin{aligned} c_C(t_1,t_2) &= \int_{-\infty}^{\infty}\int_{-\infty}^{\infty} x_1x_2 p_{X_C}(x_1,x_2,t_1,t_2)\,\mathrm{d}x_1\mathrm{d}x_2 \\ &= \int_0^{t_1} c_X(t_1-u,t_2-u)\,S_{\Delta\tau}(t_2-u)\,r(u)\,\mathrm{d}u \\ &+ \int_0^{t_1} r(u)\,\langle X(t_1-u)\rangle \int_{t_1-u}^{t_2-u} p_{\Delta\tau}(w)\int_0^{t_2-u-w} r(z) \\ &\times \langle X(t_2-u-w-z)\rangle \times S_{\Delta\tau}(t_2-u-w-z)\,\mathrm{d}z\mathrm{d}w\mathrm{d}u. \end{aligned} \tag{31}$$

Here c_X is the autocorrelation function of the driving process $X(t)$. Under the assumption of zero mean $\langle X(t)\rangle=0$, the formula simplifies conveniently, resulting in

$$c_C(t_1,t_2)=\int_0^{t_1} c_X(t_1-u,t_2-u)\,S_{\Delta\tau}(t_2-u)\,r(u)\,\mathrm{d}u. \tag{32}$$

3.2. Complete resetting—examples

3.2.1. Poissonian resetting

For the case of Poissonian resetting, $p_{\Delta\tau}(t)=r\mathrm{e}^{-rt}$, i.e. $\tilde{r}(s)=r/s+1$, and $r(t)=\delta(t)+r$, so that we have

$$\tilde{p}_{X_C}(x,s)=\tilde{p}_X(x,s+r)\,\frac{r+s}{s}=\tilde{p}_X(x,s+r)+\frac{r}{s}\tilde{p}_X(x,s+r). \tag{33}$$

Inverting the Laplace transform we get

$$p_{X_C}(x,t)=\mathrm{e}^{-rt}p_X(x,t)+r\int_0^t \mathrm{e}^{-ru}p_X(x,u)\,\mathrm{d}u, \tag{34}$$

thus retrieving the classical result from [18]. The stationary PDF is thus given by the Laplace transformed PDF of the original process via the relation

$$p_{X_C^{\mathrm{st}}}(x)=r\mathscr{L}_t\{p_X(x,t)\}(x,r). \tag{35}$$

Using formula (35), the PDF of $f(X_C^{\mathrm{st}}(t))$ for differentiable, monotonic f can again be represented as a Laplace transform,

$$p_{f(X_C^{\mathrm{st}})}(x)=\frac{r\mathscr{L}_t\{p_X(f^{-1}(x),t)\}(x,r)}{|f'(x)|}, \tag{36}$$

its mean value being

$$\langle f(X_C^{\mathrm{st}}\rangle = r\mathscr{L}_t\{\langle f(X(t))\rangle\}(r). \tag{37}$$

For a zero-mean processes, the autocorrelation takes on the form

$$c_C(t_1,t_2)=c_X(t_1,t_2)\,\mathrm{e}^{-rt_2}+r\mathrm{e}^{-rt_2}\int_0^{t_1} c_X(t_1-u,t_2-u)\,\mathrm{e}^{ru}\mathrm{d}u. \tag{38}$$

3.2.2. (a) Brownian motion

This classical case was extensively summarised in [18]. For Brownian motion $B(t)$ with MSD $\sigma^2 t$ we have $p_B(x,t) = (\sigma\sqrt{2\pi t})^{-1/2}\exp(-x^2/[2\sigma^2 t])$. Taking the Laplace transform and using equation (35) leads us to the stationary PDF

$$p_{B_C^{\mathrm{st}}}(x) = \frac{\sqrt{r}}{\sigma\sqrt{2}}\exp\left(-\frac{\sqrt{2r}}{\sigma}|x|\right), \tag{39}$$

i.e. a Laplace distribution with mean 0 and scale parameter $\sigma/\sqrt{2r}$, in accordance with the classical results. The autocorrelation function of B_C is now

$$\begin{aligned} c_C(t_1,t_2) &= \int_0^{t_1}(\delta(u)+r)\min\{t_1-u,t_2-u\}\,\mathrm{e}^{-r(t_2-u)}\mathrm{d}u \\ &= t_1\mathrm{e}^{-rt_2} + r\mathrm{e}^{-rt_2}\int_0^{t_1}(t_1-u)\,\mathrm{e}^{ru}\mathrm{d}u = \mathrm{e}^{-rt_2}\frac{\mathrm{e}^{rt_1}-1}{r} \xrightarrow{r\to 0} t_1, \end{aligned} \tag{40}$$

as expected. When $t_2 > t_1 \gg 1$ we have

$$c_C(t_1,t_2) \sim \frac{1}{r}\mathrm{e}^{-r(t_2-t_1)}. \tag{41}$$

3.2.3. (c) Lévy and α-stable processes

In general, we can claim a much stronger result for all Lévy processes (i.e. processes with stationary and independent increments) [69]. Using the well known result that the characteristic function of a Lévy process $X(t)$ has the form

$$\hat{p}_X(k,t) = \langle \mathrm{e}^{\mathrm{i}kX(t)}\rangle = \mathrm{e}^{t\Psi(k)}, \tag{42}$$

where $\Psi(k)$ is the so-called characteristic exponent [69], we now get the stationary PDF in terms of the characteristic function of such a process under Poissonian resetting,

$$\hat{p}_{X_C^{\mathrm{st}}}(k) = r\mathscr{L}_t\left\{\mathrm{e}^{t\Psi(k)}\right\}(r) = r(r-\Psi(k))^{-1}. \tag{43}$$

For α-stable processes where $\alpha \in (0,2)$ we have $\Psi(k) = -|k|^\alpha$, and we have

$$\hat{p}_{X_C^{\mathrm{st}}}(k) = r(r+|k|^\alpha)^{-1} \sim \begin{cases} |k|^{-\alpha}, & |k|\to\infty, \\ 1-|k|^\alpha, & k\to 0. \end{cases} \tag{44}$$

Using the Abelian theorem we can deduce that

$$p_{X_C^{\mathrm{st}}}(x) \overset{x\to 0}{\sim} \begin{cases} A-B|x|, & \alpha>1, \\ A|x|^{\alpha-1}, & \alpha<1 \end{cases} \tag{45}$$

and

$$p_{X_C^{\mathrm{st}}}(x) \overset{|x|\to\infty}{\sim} |x|^{-\alpha-1} \tag{46}$$

The tail behaviour does not change after introducing the resetting mechanism. Inverting this formula yields

$$p_{X_C^{\mathrm{st}}}(x) = \frac{r}{2\pi}\int_{-\infty}^{\infty}\mathrm{e}^{-\mathrm{i}kx}(r+|k|^\alpha)^{-1}\mathrm{d}k = \frac{r}{\pi}\int_0^\infty \cos(kx)(r+k^\alpha)^{-1}\mathrm{d}k. \tag{47}$$

We can evaluate this formula directly for the case $\alpha = 1$, obtaining [70]

$$p_{X_C^{\mathrm{st}}}(x) = r\sin(|x|r)\left[\frac{1}{2}-\frac{1}{\pi}\mathrm{Si}(|x|r)\right] - \frac{r}{\pi}\cos(|x|r)\,\mathrm{Ci}(|x|r), \tag{48}$$

where Ci and Si are the sine and cosine integral functions defined as

$$\mathrm{Ci}(z) = -\int_z^\infty \frac{\cos t}{t}\mathrm{d}t, \qquad \mathrm{Si}(z) = \int_0^z \frac{\sin t}{t}\mathrm{d}t. \tag{49}$$

In this case, we have the so-called Cauchy process. We can see a comparison of the theoretical result with the simulations in figure 3.

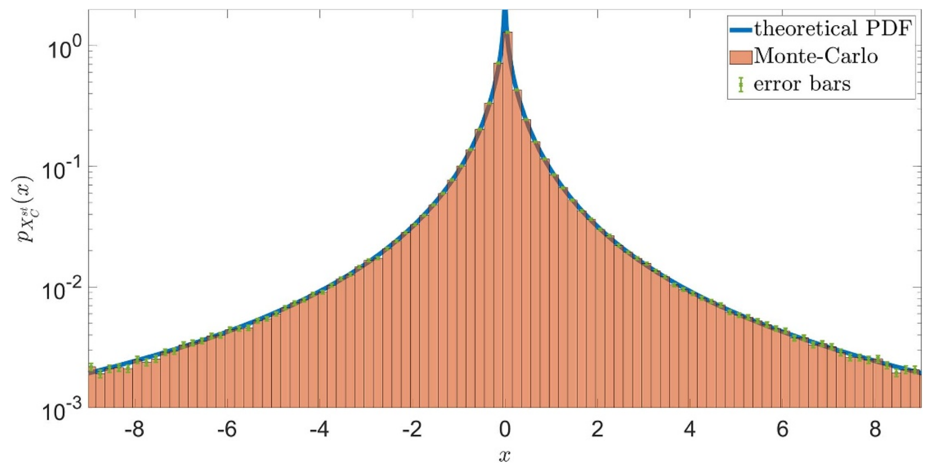

Figure 3. Comparison of the theoretical result (48) for the PDF of the stationary distribution of Cauchy process with Poissonian resetting. Here we used $t = 10^2$, $r = 2$ and the Monte-Carlo sample size 5×10^5. The error bars show the standard deviation as deduced from the Monte-Carlo estimation for each bar of the histogram. The error bars are relatively small due to high precision of the simulated result.

3.2.4. (b) SBM

SBM is a Gaussian process with mean 0 and $\langle B_\alpha(s)B_\alpha(t)\rangle = K_\alpha \min\{s^\alpha, t^\alpha\}$. The paths can be simulated using the Cholesky decomposition or in a stepwise manner using the Itô formulation

$$\mathrm{d}B_\alpha(t) = \sqrt{K_\alpha \alpha} t^{(\alpha-1)/2} \mathrm{d}B(t) \implies B_\alpha(t) = \sqrt{K_\alpha \alpha} \int_0^t s^{(\alpha-1)/2} \mathrm{d}B(s). \tag{50}$$

We have that [44, 67, 68]

$$p_{B_\alpha}(x,t) = \frac{1}{\sqrt{4\pi K_\alpha t^\alpha}} \exp\left(-\frac{x^2}{4K_\alpha t^\alpha}\right). \tag{51}$$

To calculate the MSD from the stationary PDF under resetting we again need the Laplace transform of $\langle B_\alpha^2(t)\rangle$, i.e.

$$\left\langle (B_\alpha^{st})_C^2 \right\rangle = 2K_\alpha r \mathscr{L}_t\{t^\alpha\}(r) = \frac{2K_\alpha \Gamma(\alpha+1)}{r^\alpha}. \tag{52}$$

With the knowledge that $c_{B_\alpha}(t_1,t_2) = 2K_\alpha(\min\{t_1,t_2\})^\alpha$, we obtain the autocorrelation function

$$\begin{aligned} c_C(t_1,t_2) &= 2K_\alpha t_1^\alpha \mathrm{e}^{-rt_2} + 2K_\alpha r \mathrm{e}^{-rt_2} \int_0^{t_1} (t_1-u)^\alpha \mathrm{e}^{ru} \mathrm{d}u \\ &= 2K_\alpha t_1^\alpha \mathrm{e}^{-rt_2} + 2K_\alpha r^{-\alpha} \mathrm{e}^{-r(t_2-t_1)} \int_0^{rt_1} u^\alpha \mathrm{e}^{-u} \mathrm{d}u \\ &= 2K_\alpha t_1^\alpha \mathrm{e}^{-rt_2} + 2K_\alpha r^{-\alpha} \mathrm{e}^{-r(t_2-t_1)} \gamma(\alpha+1, rt_1), \end{aligned} \tag{53}$$

where γ is the lower incomplete gamma function. Taking the limit $r \to 0$ and utilising the asymptotic property of the lower gamma function, $\gamma(s,x) \sim x^s/s$ for small x, we see that the autocorrelation simplifies to the standard SBM case. Asymptotically for $t_2 > t_1 \gg 1$ we have

$$c_C(t_1,t_2) \sim \frac{2K_\alpha \Gamma(\alpha+1) \mathrm{e}^{-r(t_2-t_1)}}{r^\alpha} \overset{\alpha \to 1}{\to} \frac{\mathrm{e}^{-r(t_2-t_1)}}{r}. \tag{54}$$

We see that when $\alpha = 1$ the result simplifies to the previous result for standard Brownian motion. To calculate the stationary PDF we take the Laplace transform of $p_{B_\alpha}(x,t)$,

$$\mathscr{L}_t\{p_{B_\alpha}\}(x,r) = \frac{1}{\sqrt{4\pi K_\alpha}} \int_0^\infty t^{-\alpha/2} \exp\left(-\frac{x^2}{4K_\alpha t^\alpha} - rt\right) \mathrm{d}t. \tag{55}$$

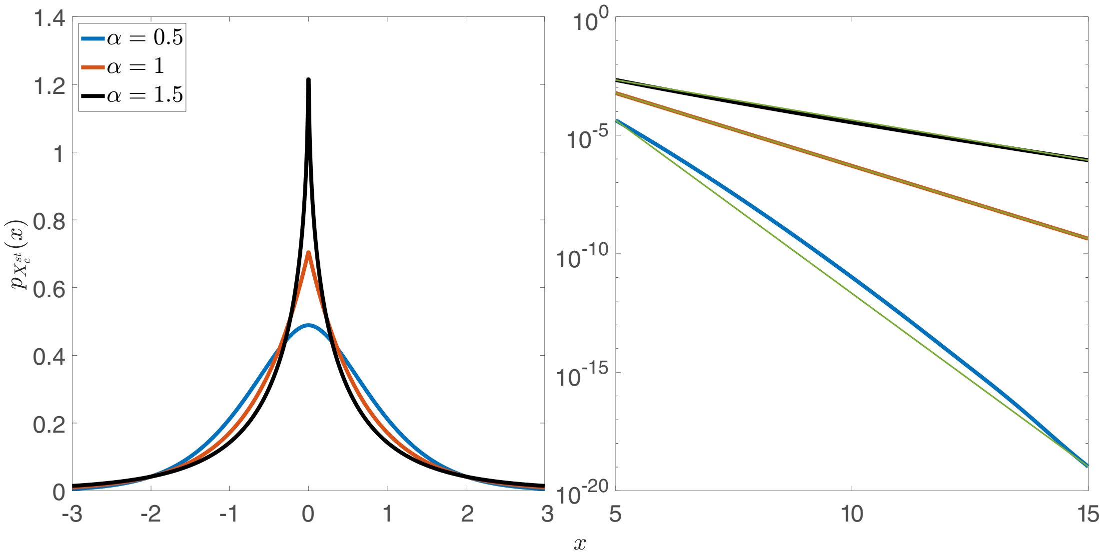

Figure 4. Comparison of the stationary PDFs (57) of SBM under Poissonian resetting, with $K = 1/2$ and $r = 1$. We notice a difference in the tail behaviour of the PDFs, shown on the right panel in which we present it using a log-linear scale with green straight lines for reference. For $\alpha \geqslant 1$ the PDF behaves exponentially, while for $\alpha < 1$ it has clearly lighter tails.

After appropriate substitutions we identify equation (55) as the Krätzel Z-function [71, 72],

$$Z_\rho^\nu(x) = \int_0^\infty t^{\nu-1} \mathrm{e}^{-t^\rho - x/t} \mathrm{d}t. \tag{56}$$

Consequently, we get

$$p_{B^{st}_{\alpha C}}(x) = r\left(\frac{x^2}{4K_\alpha}\right)^{1/\alpha} \left(\sqrt{\pi}|x|\right)^{-1} Z_\alpha^{\alpha/2-1}\left(r\left(\frac{x^2}{4K_\alpha}\right)^{1/\alpha}\right). \tag{57}$$

We show a comparison of the stationary PDFs in figure 4. Notice the behaviour of the PDF at $x = 0$. In this subdiffusive case, the process tends to drift very quickly before slowing down its movement. This is the reason why we see a smooth PDF at the resetting point $x = 0$—the trajectories do not cluster together with the ones just after the reset. For $\alpha \geqslant 1$ the normal or super-diffusive trajectories do not leave the resetting point quickly enough and mix together with the ones just after the reset. This creates a substantial probability mass at the origin that creates a non-differentiability of the PDF.

A change of the behaviour of the process at $\alpha = 1$ can also be seen in the tail behaviour of the PDF. For the subdiffusive case, the tail behaves sub-exponentially, for the normal one exponentially, while for the superdiffusive case it decays super-exponentially. This is in line with results from https://arxiv.org/abs/2112.02928, where we see, that

$$Z_\alpha^{\alpha/2-1}(z) \overset{z\to\infty}{\sim} \frac{\sqrt{2\pi}}{\alpha+1} \alpha^{\frac{1-\alpha}{2(\alpha+1)}} z^{\alpha+1} \mathrm{e}^{-\left(1+\frac{1}{\alpha}\right)\left(\frac{z}{\alpha}\right)^{1+\frac{1}{\alpha}}}. \tag{58}$$

This gives us, that

$$p_{B^{st}_{\alpha C}}(x) \overset{|x|\to\infty}{\sim} |x|^{\frac{1-\alpha}{\alpha+1}} \exp\left(-\left[\frac{x^2 r^\alpha}{4K_\alpha}\right]^{\frac{1}{\alpha+1}} \left[\alpha^{\frac{1}{\alpha+1}} + \alpha^{-\frac{\alpha}{\alpha+1}}\right]\right) \tag{59}$$

where $B(r,\alpha) = C(r)\alpha^{\frac{1}{1+\alpha}} + \alpha^{-\frac{\alpha}{1+\alpha}}$. Alternatively, a standard Laplace method can be utilised to approximate the integral in (55) as in [44], resulting in

$$p_{B_{\alpha C}}(x,t) \overset{t\to\infty}{\sim} \frac{r\sqrt{2}}{\sqrt{\alpha(\alpha+1)}} \left(\frac{\alpha}{4K_\alpha r}\right)^{\frac{1}{\alpha+1}} |x|^{\frac{1-\alpha}{\alpha+1}} \exp\left(-\left[\frac{x^2 r^\alpha}{4K_\alpha}\right]^{\frac{1}{\alpha+1}} \left[\alpha^{\frac{1}{\alpha+1}} + \alpha^{-\frac{\alpha}{\alpha+1}}\right]\right). \tag{60}$$

This approach has the benefit of simplicity, but it generates some inaccuracies in further calculations. As it uses a Gaussian approximation, this method is best when α is close to 1. It recovers the tail behaviour of the function very well.

3.2.5. Mixture of exponentially distributed resetting times

Now let us choose $\Delta\tau$ as a mixture of exponentials, i.e. $\Delta\tau$ has the PDF $p_{\Delta\tau}(t)=\int_0^\infty r\mathrm{e}^{-rt}\mathrm{d}F_R(r)$, where F_R is some cumulative density function (CDF). It can be interpreted as an exponential distribution $\mathcal{E}(R)$ with random parameter R having the distribution function F_R. Such distributions have found a number of important applications in physics and related sciences. Mixtures of exponential distributions are used in physics in the modelling of systems exhibiting multiple processes with different characteristic time scales or rates, especially when phenomena involve multiple decay rates, heterogeneous processes, or composite systems. They often appear when simple single-exponential models fail to capture the observed behaviour, e.g. in complex, stochastic, or disordered systems. Examples of areas in physics, where mixtures of exponential distributions are applied include: time delay of electrical breakdown along with the generalised relation for the effective electron yield [73]; climatology, in the modelling of rainfall processes, highlighting the effectiveness of mixed models in capturing rainfall variability [74]; and the study of human behaviour, where mixtures of exponential distributions have been employed to model inter-event times more accurately, capturing the variability in human activity patterns [75]. Sums of exponentials were also used in [76] to accurately approximate the fractional Langevin equation in the framework of Markovian embedding techniques. In [77] these distributions were used to retrieve the fraction of ground lightning flashes in a set of flashes observed from a satellite lightning image. In [78] a mixed exponential distribution was used to evaluate extreme-value rainfall. In [79] the authors introduced a jump diffusion model with mixed exponential jumps and applied it to option pricing. In [80] it was used to describe temperature fluctuations for heavy ion collisions. Finally, in [81] the authors modelled rainfall arrivals for different rainfall depth distributions, in particular for mixed exponentials. We also underline the practical importance of these distributions, as such mixture-exponential distributions are well suited for calculations. Moreover, they can be used to approximate other, possibly more complicated distributions of $\Delta\tau$, see section 4.2.4 and also [82].

Let us now calculate the PDF p_{X_C} corresponding to mixture-exponential resetting times. Due to the linearity of the Laplace transform and the exponential form of the summands, the calculations can be conducted in a similar manner, yielding

$$\tilde{p}_{X_C}(x,s)=\frac{\int_0^\infty \tilde{p}_X(x,s+r)\,\mathrm{d}F_R(r)}{1-\int_0^\infty \frac{r}{r+s}\mathrm{d}F_R(r)}=\frac{\mathbb{E}\left(\tilde{p}_X(x,s+R)\right)}{1-\mathbb{E}\left(\frac{R}{R+s}\right)}=\frac{\mathbb{E}\left(p_X(x,s+R)\right)}{\mathbb{E}\left(\frac{s}{R+s}\right)}. \tag{61}$$

We see that if R is degenerate and equal to a deterministic constant value, the result reduces to the previous Poissonian case.

Now let us consider a special case and assume that $p_R(r)=\sum_{i=1}^n p_i\delta(r-r_i)$, with $p_i,r_i\geqslant 0$, $n\in\mathbb{N}_+$, and $\sum_{i=1}^n p_i=1$, i.e. we choose a discrete distribution of R. In this case our PDF takes on the form

$$\tilde{p}_{X_C}(x,s)=\frac{\sum_{i=1}^n p_i\tilde{p}_X(x,s+r_i)}{s\sum_{i=1}^n\frac{p_i}{r_i+s}}. \tag{62}$$

This formula can be inverted in Laplace space in the limit $t\to\infty$, yielding a weighted combination of the terms from the standard Poissonian resetting. Using standard Abelian and Tauberian theorems we can investigate the limiting behaviour of $p_{X_C}(x,t)$ for large t by studying the behaviour of $p_{X_C}(x,s)$ for small s [83]. We can thus expand the sum in the denominator of (62) using the first term of its Maclaurin expansion,

$$\left(\sum_{i=1}^n\frac{p_i}{r_i+s}\right)^{-1}=\left(\sum_{i=1}^n\frac{p_i}{r_i}\right)^{-1}+O(s). \tag{63}$$

After plugging approximation (63) into equation (62) and inverting the transform, for large t the PDF behaves as

$$p_{X_C}(x,t)\overset{t\to\infty}{\sim}\left(\sum_{i=1}^n\frac{p_i}{r_i}\right)^{-1}\sum_{i=1}^n p_i\int_0^t \mathrm{e}^{-r_iu}p_X(x,u)\,\mathrm{d}u. \tag{64}$$

Letting $t\to\infty$ we arrive at the stationary PDF

$$p_{X_C^{\mathrm{st}}}(x)=\left(\sum_{i=1}^n\frac{p_i}{r_i}\right)^{-1}\sum_{i=1}^n p_i\mathscr{L}_t\{p_X(x,t)\}(r_i). \tag{65}$$

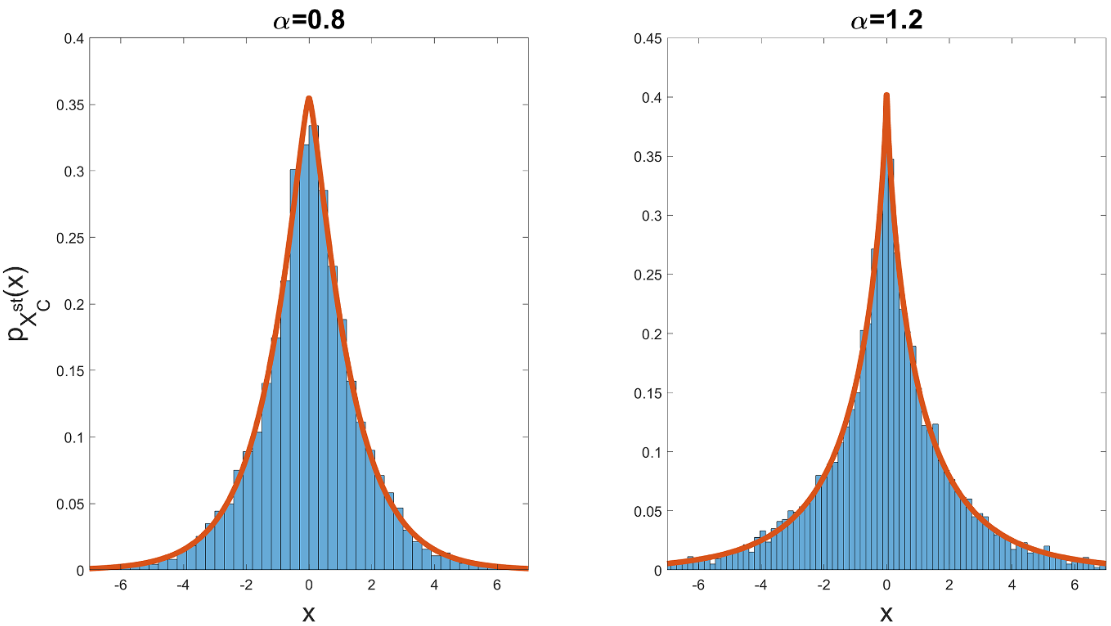

Figure 5. Comparison of MC simulations ($N = 10^4$) with analytical results for the stationary PDF (65) for SBM with mixed-exponential resetting with $\mathbf{r} = (1/2, 1/5, 1)$, $\mathbf{p} = (1/2, 1/4, 1/4)$. We again notice that for $\alpha < 1$ the non-differentiability at $x = 0$ appears to disappear.

When X is a Brownian motion the above stationary PDF reads

$$p_{X_C^{st}}(x) = \left(\sum_{i=1}^{n} \frac{p_i}{r_i}\right)^{-1} \sum_{i=1}^{n} p_i \frac{1}{\sqrt{2r_i}} \exp\left(-\sqrt{2r_i}|x|\right). \tag{66}$$

We notice that this does not yield a simple convex combination of random variables with Laplace distribution, as the scaling factors are now non-linearly intertwined via the first sum. In the case $n = 1$ it does simplify to the previous Poissonian case.

The numerical results in the long time limit when X represents an SBM are shown in figure 5. The simulations confirm our calculations, as the histograms of the trajectories is near-perfectly estimated by the derived stationary PDFs in the sub- and superdiffusive cases. The explicit form of the PDF can be simply derived using equations (65) and (57).

3.3. PDF for incomplete resetting

We now calculate the PDF corresponding to the process X with incomplete resetting. We start with the process $X_P(t)$ conditioned on $N(t)$. We then have

$$\begin{aligned} X_P(t) \,|\, (N(t) = n) &= X(t) - \sum_{i=0}^{\infty} X(\tau_i) \mathbf{1}_{N(t)=i} | (N(t) = n) \\ &= X(t) - X(\tau_n) \,|\, (N(t) = n). \end{aligned} \tag{67}$$

We again use the law of total probability for the PDF $p_{X_P}(x,t)$,

$$\begin{aligned} p_{X_P}(x,t)\,\mathrm{d}x &= \mathbb{P}(X_P(t) \in (x, x+\mathrm{d}x)) \\ &= \sum_{n=0}^{\infty} \mathbb{P}(X_P(t) \in (x, x+\mathrm{d}x), N(t) = n) \\ &= \sum_{n=0}^{\infty} \mathbb{P}(X(t) - X(\tau_n) \in (x, x+\mathrm{d}x), N(t) = n). \end{aligned} \tag{68}$$

Again using the fact that the events $N(t) = n$ and $0 \leqslant t - \tau_n < \Delta\tau_{n+1}$ are equivalent, we obtain

$$
\begin{aligned}
p_{X_P}(x,t)\,\mathrm{d}x &= \sum_{n=0}^{\infty} \mathbb{P}\left(X(t) - X(\tau_n) \in (x, x+\mathrm{d}x), 0 \leqslant t - \tau_n < \Delta\tau_{n+1}\right) \\
&= \sum_{n=0}^{\infty} \int_0^t \mathbb{P}\left(X(t) - X(u) \in (x, x+\mathrm{d}x), 0 \leqslant t - u < \Delta\tau_{n+1}\right) p_{\tau_n}(u)\,\mathrm{d}u \\
&= \int_0^t \mathbb{P}\left(X(t) - X(u) \in (x, x+\mathrm{d}x)\right) S_{\Delta\tau}(t-u)\, r(u)\,\mathrm{d}u. \qquad (69)
\end{aligned}
$$

Here, we used the law of total probability with respect to the τ_n and used the definition (17) of $r(t)$.

Let us now define the PDF $p_{I_X}(x,u,t)$ of the process $I_X(u,t) = X(t) - X(u)$ for $t \geqslant u$. If the process has stationary increments, then $I_X(u,t) \overset{D}{=} X(t-u)$ and the PDF simplifies to the complete resetting case. We then have

$$
p_{X_P}(x,t) = \int_0^t r(u)\, p_{I_X}(x,u,t)\, S_{\Delta\tau}(t-u)\,\mathrm{d}u, \qquad (70)
$$

or

$$
\begin{aligned}
p_{X_P}(x,t) &= \int_0^t r(u)\, p_{I_X}(x, t-u)\, S_{\Delta\tau}(t-u)\,\mathrm{d}u \\
&= \int_0^t r(u)\, p_X(x, t-u)\, S_{\Delta\tau}(t-u)\,\mathrm{d}u = r(t) \overset{t}{*} p_X(x,t)\, S_{\Delta\tau}(t), \qquad (71)
\end{aligned}
$$

in the case of stationary increments, where we used $p_{I_X}(x,u,t) = p_{I_X}(x,t-u) = p_X(x,t-u)$.

3.4. Incomplete resetting—examples

3.4.1. Poissonian resetting

We employ $R(t) = \mathrm{e}^{-rt}$ with $r(t) = \delta(t) + r$. Using (70) we then have

$$
p_{X_P}(x,t) = \mathrm{e}^{-rt} p_X(x,t) + r\mathrm{e}^{-rt} \int_0^t \mathrm{e}^{ru} p_{I_X}(x,u,t)\,\mathrm{d}u. \qquad (72)
$$

After a change of variables we see that

$$
p_{X_P}(x,t) = \mathrm{e}^{-rt} p_X(x,t) + r \int_0^t \mathrm{e}^{-ru} p_{I_X}(x, t-u, t)\,\mathrm{d}u. \qquad (73)
$$

To calculate the MSD of this process we use the definition

$$
\langle X_P^2(t)\rangle = \mathrm{e}^{-rt}\langle X^2(t)\rangle + r\int_0^t \mathrm{e}^{-ru}\langle I_X^2(t-u,t)\rangle \mathrm{d}u. \qquad (74)
$$

Assuming that the MSD of the underlying process displays at most algebraic growth, we can see that this formula can be asymptotically approximated as

$$
\langle X_P^2(t)\rangle \overset{t\to\infty}{\sim} r\int_0^t \mathrm{e}^{-ru}\langle I_X^2(t-u,t)\rangle \mathrm{d}u. \qquad (75)
$$

3.4.2. SBM

The PDF of I_{B_α} is well known and given by

$$
p_{I_{B_\alpha}}(x,u,t) = \frac{1}{\sqrt{4\pi K_\alpha (t^\alpha - u^\alpha)}} \exp\left(-\frac{x^2}{4K_\alpha (t^\alpha - u^\alpha)}\right). \qquad (76)
$$

The variance of $I_{B_\alpha}(t-u,t)$ is $2K_\alpha\left(t^\alpha - (t-u)^\alpha\right)$. Substituting this expression into (75) we get

$$
\langle B_{\alpha P}^{\,2}(t)\rangle \overset{t\to\infty}{\sim} \frac{2K_\alpha t^{\alpha-1}}{r}. \qquad (77)
$$

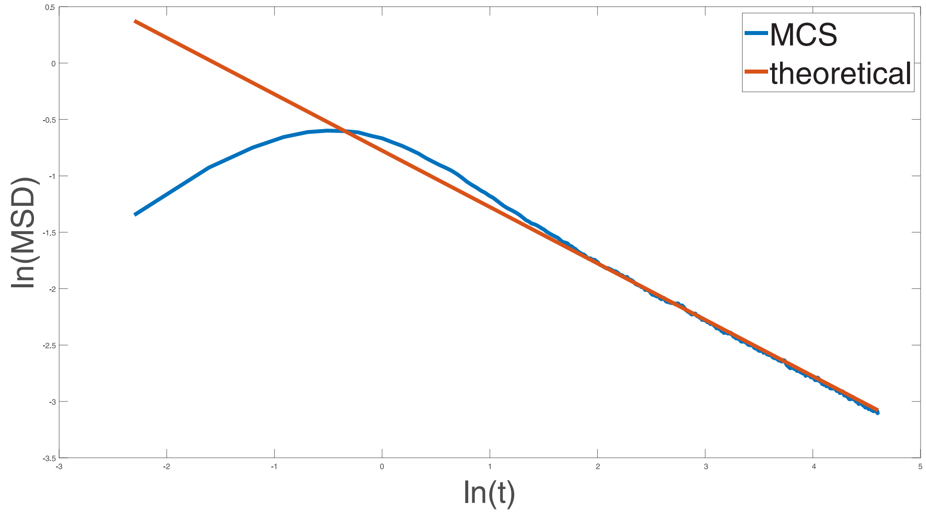

Figure 6. Comparison of Monte-Carlo simulations based on 10^5 samples for the MSD of SBM under incomplete resetting with the theoretical asymptotical result for the case $\alpha = 1/2$. The MSD behaves as $t^{\alpha-1}$, as predicted by the analytical result (77).

Consequently, this process can achieve a stationary state only in the case $\alpha = 1$, which is exactly the case of Brownian motion[6]. Subdiffusive SBM will converge to a degenerate stochastic process $B_{\alpha P}^{st} = 0$, SBM in the superdiffusive case $\alpha \in (1,2)$ with resetting will behave subdiffusively at long times. This result is expected, as the scaling exponent α controls the volatility of the increments. For $\alpha < 1$ the volatility increases slower than linearly, while the rate of resetting is always constant and the number of resets in time grows linearly. For $\alpha = 1$ both mechanisms behave linearly and their impact complements each other, thus achieving a non-degenerate stationary state. The case $\alpha > 1$ displays a super-linear growth in the volatility that the resetting mechanism cannot compensate. This behaviour is in sharp contrast to the complete resetting case, where the stationary states are more common, as the memory is erased and the displacement volatility returns to its initial state. In figure 6 we can see a numerical confirmation of the result. The theoretical result $t^{\alpha-1}$ for the long-time behaviour of the MSD exactly matches the simulations. We see an initial increase of the MSD estimated from Monte-Carlo simulations, before the subdiffusive behaviour of the trajectories is suppressed by the resetting mechanism.

4. First-passage behaviour

We now consider the first-passage dynamics of the process for the different resetting scenarios based on our series representation approach. Concretely, we derive the first-passage time density (FPTD) in Laplace space and its mean. We explicitly derive results for the first-passage dynamics for specific cases and also demonstrate that these reduce to already known special cases. Finally, we introduce an approximation tool for the case when the PDF of inter-resetting times is only partially known. A typical trajectory of a process under SR with highlighted first-passage event is shown in figure 7.

4.1. Complete resetting—FPTD

In this section we will derive the FPT PDF for the case of complete resetting. Consider the FPT $T_a = \inf\{t > 0 | X_C(t) \geqslant a > 0\}$, the first time the process with complete resetting hits or surpasses a certain level a. We use the auxiliary random variable $I_a = \min\left\{i | \exists_t X_i(t-\tau_i)\mathbf{1}_{N(t)=i} \geqslant a\right\}$, the index of the time interval during which the first-passage event takes place, i.e. $\{I_a = i\} = \{\tau_i \leqslant T_a < \tau_{i+1}\}$. From this definition we see that $\tau_{I_a} \leqslant T_a < \tau_{I_a+1}$. We denote the probability that the driving process X will hit or surpass the level a on an inter-resetting interval $\Delta\tau$ as

$$p = \mathbb{P}(T_a' \leqslant \Delta\tau) = \int_0^\infty \mathbb{P}(T_a' \leqslant u) p_{\Delta\tau}(u)\,\mathrm{d}t = \int_0^\infty F_{T_a'}(u) p_{\Delta\tau}(u)\,\mathrm{d}u. \tag{78}$$

The probability that the process will not hit or surpass the level a then is $q = 1 - p = \int_0^\infty S_{T_a'}(u) p_{\Delta\tau}(u)\mathrm{d}u$. Here, $p_{\Delta\tau}$ is the PDF of $\Delta\tau$, $T_a' = \inf\{t | X(t) \geqslant a\}$; $F_{T_a'}$ is the CDF of T_a', and $S_{T_a'} = 1 - F_{T_a'}$ is the survival

[6] A similar case is found for confined SBM in an external potential: the MSD of subdiffusive SBM decays as function of time, and vice versa for superdiffusive SBM. Only the normal-diffusive case $\alpha = 1$ assumes a stationary plateau [68].

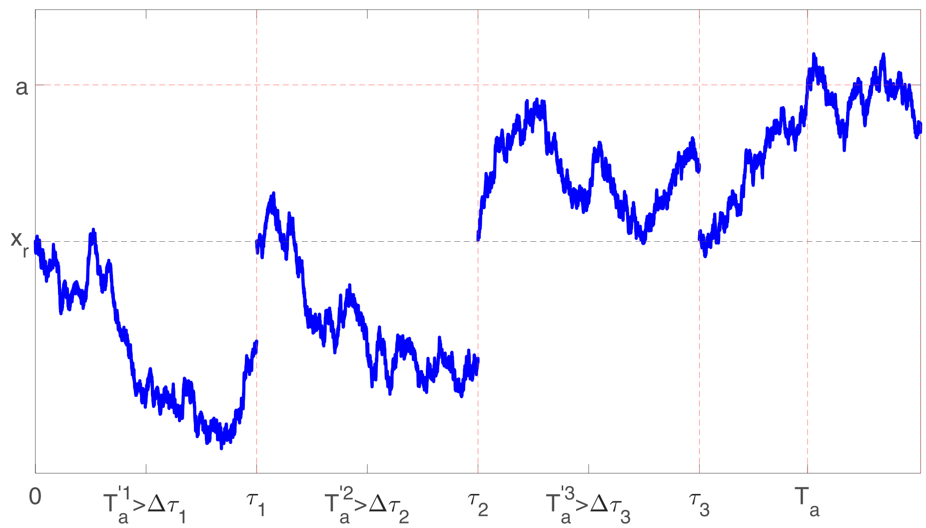

Figure 7. Visualisation of the first-passage event at $x = a$ for a stochastic process with complete resetting. We introduce a partitioning of the time axis with respect to the resetting times. This allows us to use properties of the FPT of the underlying parental process, see text for details.

probability. We assume that $\mathbb{P}(T'_a < \infty) > 0$ to avoid degenerate cases. The mean of T'_a may be infinite, as it is in the case of Brownian motion. We also notice that $T_a \overset{D}{=} \tau_{I_a} + T'_a | T'_a < \Delta\tau$.

Now we calculate the PDF of τ_{I_a} using IID copies $T_a'^{i}$ of T'_a,

$$p_{\tau_{I_a}}(t)\,\mathrm{d}t = \sum_{k=0}^{\infty} \mathbb{P}\left(\tau_{I_a} \in (t, t+\mathrm{d}t), I_a = k\right). \tag{79}$$

We denote the terms in the sum (79) as $P_k(t)$. Analysing them separately we obtain

$$\begin{aligned} P_k(t) &= \mathbb{P}\left(\tau_k \in (t, t+\mathrm{d}t), \tau_k \leqslant T_a < \tau_{k+1}\right) \\ &= \mathbb{P}\left(\tau_k \in (t, t+\mathrm{d}t), 0 \leqslant T_a - \tau_k, T_a - \tau_k < \Delta\tau_{k+1}\right). \end{aligned} \tag{80}$$

Here we used the definition of I_a and the definition of τ_{k+1} as the sum of inter-resetting times. The event $I_a = k$ can be expressed in terms of the independent $T_a'^{i}$ variables. Note that $T_a'^{i} \geqslant \Delta\tau_i$ for $i \leqslant k$, as on these intervals the processes has not crossed the barrier a. Meanwhile, on the $(k+1)$th interval we have $T_a'^{k+1} < \Delta\tau_{k+1}$, since on the last interval the process reached the barrier a within a time period that is shorter than the corresponding inter-resetting time. Therefore

$$P_k(t) = \mathbb{P}\left(\sum_{i=1}^{k} \Delta\tau_i \in (t, t+\mathrm{d}t), \underset{1\leqslant i\leqslant k}{\forall} T_a'^{i} \geqslant \Delta\tau_i, T_a'^{k+1} < \Delta\tau_{k+1}\right). \tag{81}$$

This allows us to extract $\Delta\tau_k$ and use the law of total expectation to get

$$\begin{aligned} P_k(t) = \int_0^t p_{\Delta\tau}(u)\mathbb{P}\Bigg(&\sum_{i=1}^{k-1}\Delta\tau_i \in (t-u, t-u+\mathrm{d}t), \\ &\underset{1\leqslant i\leqslant k-1}{\forall} T_a'^{i} \geqslant \Delta\tau_i, T_a'^{k} \geqslant u, T_a'^{k+1} < \Delta\tau_{k+1}\Bigg)\mathrm{d}u. \end{aligned} \tag{82}$$

We note that the event $T_a'^{k} \geqslant u$ is independent from all other events in the expression above, resulting in

$$\begin{aligned} P_k(t) = \int_0^t p_{\Delta\tau}(u) S_{T'_a}(u)\mathbb{P}\Bigg(&\sum_{i=1}^{k-1}\Delta\tau_i \in (t-u, t-u+\mathrm{d}t), \\ &\forall_{1\leqslant i\leqslant k-1} T_a'^{i} \geqslant \Delta\tau_i, T_a'^{k} < \Delta\tau_k\Bigg)\mathrm{d}u. \end{aligned} \tag{83}$$

The probability in the integral is in fact $P_{k-1}(t)$. After recognising the form of the integral as a convolution we rephrase it in the form

$$\begin{aligned} P_k(t) &= \int_0^t p_{\Delta\tau}(u) S_{T'_a}(u) \mathbb{P}(\tau_{I_a} \in (t-u, t-u+\mathrm{d}t), I_a = k-1) \,\mathrm{d}u \\ &= p_{\Delta\tau}(t) S_{T'_a}(t) \overset{t}{*} \mathbb{P}(\tau_{I_a} \in (t, t+\mathrm{d}t), I_a = k-1) \\ &= p_{\Delta\tau}(t) S_{T'_a}(t) \overset{t}{*} P_{k-1}(t). \end{aligned} \tag{84}$$

Comparing the first and the last lines above we conclude that

$$\underset{k\in\mathbb{N}_+}{\forall} p_{\Delta\tau}(t) S_{T'_a}(t) \overset{t}{*} P_k(t) = p_{\Delta\tau}(t) S_{T'_a}(t) \overset{t}{*} P_{k-1}(t). \tag{85}$$

This implies that for all $k \in \mathbb{N}_+$, $P_k(t)$ is a convolution of

$$\begin{aligned} P_0(t) &= \mathbb{P}(\tau_0 \in (t, t+\mathrm{d}t), I_a = 0) \\ &= \mathbb{P}(0 \in (t, t+\mathrm{d}t), I_a = 0) \\ &= \delta(t) \mathbb{P}(I_a = 0) \,\mathrm{d}t = \delta(t) \mathbb{P}(T_a < \tau_1) \,\mathrm{d}t \\ &= \delta(t) \mathbb{P}(T'_a < \Delta\tau) \,\mathrm{d}t = p\delta(t) \,\mathrm{d}t \end{aligned} \tag{86}$$

with a k-fold convolution of $p_{\Delta\tau}(t) S_{T'_a}(t)$, i.e.

$$P_k(t) = p \left(p_{\Delta\tau}(t) S_{T'_a}(t)\right)^{(*k)} \mathrm{d}t. \tag{87}$$

Plugging this result back into equation (79) we obtain

$$p_{\tau_{I_a}}(t) = p \sum_{k=0}^{\infty} \left(p_{\Delta\tau}(t) S_{T'_a}(t)\right)^{(*k)}. \tag{88}$$

For further calculations we switch to Laplace space to get

$$\tilde{p}_{\tau_{I_a}}(s) = p \sum_{k=0}^{\infty} \left(\mathscr{L}_t\{p_{\Delta\tau} S_{T'_a}\}(s)\right)^k = \frac{p}{1 - \mathscr{L}_t\{p_{\Delta\tau} S_{T'_a}\}(s)}. \tag{89}$$

With this result for the PDF of τ_{I_a} we can now use the aforementioned property $T_a \overset{D}{=} \tau_{I_a} + T'_a | (T'_a < \Delta\tau)$ to calculate the PDF of this sum via multiplication in Laplace space. The distribution of $T'_a | (T'_a < \Delta\tau)$ can then be easily obtained using the law of total probability,

$$\begin{aligned} p_{T'_a|T'_a<\Delta\tau}(t) \,\mathrm{d}t &= \mathbb{P}(T'_a \in (t, t+\mathrm{d}t) | T'_a < \Delta\tau) \\ &= \frac{1}{\mathbb{P}(T'_a < \Delta\tau)} \int_0^{\infty} p_{\Delta\tau}(u) \mathbb{P}(T'_a \in (t, t+\mathrm{d}t), T'_a < u) \,\mathrm{d}u \\ &= \frac{1}{p} \int_t^{\infty} p_{\Delta\tau}(u) p_{T'_a}(t) \,\mathrm{d}u\mathrm{d}t = \frac{1}{p} S_{\Delta\tau}(t) p_{T'_a}(t) \,\mathrm{d}t, \end{aligned} \tag{90}$$

resulting in $p_{T'_a|T'_a<\Delta\tau}(t) = (1/p) S_{\Delta\tau}(t) p_{T'_a}(t)$. We can now explicitly express p_{T_a} in Laplace space as

$$\tilde{p}_{T_a}(s) = \frac{\mathscr{L}_t\{S_{\Delta\tau} p_{T'_a}\}(s)}{1 - \mathscr{L}_t\{p_{\Delta\tau} S_{T'_a}\}(s)}. \tag{91}$$

The mean of T_a can be obtained via differentiation of expression (91), i.e.

$$\tilde{p}'_{T_a}(s) = \frac{\frac{\mathrm{d}}{\mathrm{d}s} \mathscr{L}_t\{S_{\Delta\tau} p_{T'_a}\}(s)}{1 - \mathscr{L}_t\{p_{\Delta\tau} S_{T'_a}\}(s)} + \frac{\mathscr{L}_t\{S_{\Delta\tau} p_{T'_a}\}(s) \frac{\mathrm{d}}{\mathrm{d}s} \mathscr{L}_t\{p_{\Delta\tau} S_{T'_a}\}(s)}{\left(1 - \mathscr{L}_t\{p_{\Delta\tau} S_{T'_a}\}(s)\right)^2}. \tag{92}$$

Calculating every component separately, we first have

$$\begin{aligned}\frac{\mathrm{d}}{\mathrm{d}s}\mathscr{L}_t\{S_{\Delta\tau}p_{T_a'}\}(s) &= \frac{\mathrm{d}}{\mathrm{d}s}\int_0^\infty \mathrm{e}^{-st}S_{\Delta\tau}(t)\,p_{T_a'}(t)\,\mathrm{d}t\\ &= -\int_0^\infty t\mathrm{e}^{-st}S_{\Delta\tau}(t)\,p_{T_a'}(t)\,\mathrm{d}t\\ &\overset{s\to 0}{\to} -\int_0^\infty tS_{\Delta\tau}(t)\,p_{T_a'}(t)\,\mathrm{d}t.\end{aligned} \tag{93}$$

For the next term, we get

$$\begin{aligned}\frac{\mathrm{d}}{\mathrm{d}s}\mathscr{L}_t\{S_{T_a'}p_{S_{\Delta\tau}}\}(s) &= \frac{\mathrm{d}}{\mathrm{d}s}\int_0^\infty \mathrm{e}^{-st}S_{T_a'}(t)\,p_{\Delta\tau}(t)\,\mathrm{d}t\\ &= -\int_0^\infty t\mathrm{e}^{-st}S_{T_a'}(t)\,p_{\Delta\tau}(t)\,\mathrm{d}t\\ &\overset{s\to 0}{\to} -\int_0^\infty tS_{T_a'}(t)\,p_{\Delta\tau}(t)\,\mathrm{d}t.\end{aligned} \tag{94}$$

We also have

$$\begin{aligned}1-\mathscr{L}_t\{p_{\Delta\tau}S_{T_a'}\}(s) &\overset{s\to 0}{\to} 1-\int_0^\infty p_{\Delta\tau}(t)\,S_{T_a'}(t)\,\mathrm{d}t\\ &= \int_0^\infty p_{\Delta\tau}(t)\,\mathrm{d}t-\int_0^\infty p_{\Delta\tau}(t)\,S_{T_a'}(t)\,\mathrm{d}t\\ &= \int_0^\infty p_{\Delta\tau}(t)\left(1-S_{T_a'}(t)\right)\mathrm{d}t\\ &= \int_0^\infty p_{\Delta\tau}(t)\,F_{T_a'}\mathrm{d}t,\end{aligned} \tag{95}$$

where we used the property $S_{T_a'}(t)=1-F_{T_a'}(t)$. Lastly, we have

$$\begin{aligned}\mathscr{L}_t\{p_{T_a'}S_{\Delta\tau}\}(s) &\overset{s\to 0}{\to} \int_0^\infty p_{T_a'}(t)\,S_{\Delta\tau}(t)\,\mathrm{d}t=\int_0^\infty S_{\Delta\tau}(t)\,\mathrm{d}F_{T_a'}(t)\\ &= S_{\Delta\tau}(t)\,F_{T_a'}(t)\Big|_0^\infty-\int_0^\infty F_{T_a'}(t)\,\mathrm{d}S_{\Delta\tau}(t)\\ &= \int_0^\infty F_{T_a'}(t)\,p_{\Delta\tau}(t)\,\mathrm{d}t,\end{aligned} \tag{96}$$

where we used the property $S'_{\Delta\tau}(t)=-p_{\Delta\tau}(t)$ and the fact that the integration limits vanish due to the boundedness of $F_{T_a'}, S_{\Delta\tau}$ and conditions $\lim_{t\to\infty} S_{\Delta\tau}(t)=F_{T_a'}(0)=0$. Combining the results (93)–(96) we obtain

$$\tilde{p}'_{T_a}(s)\Big|_{s\downarrow 0}=-\frac{\int_0^\infty t\left(S_{\Delta\tau}(t)\,p_{T_a'}(t)+S_{T_a'}(t)\,p_{\Delta\tau}(t)\right)\mathrm{d}t}{\int_0^\infty p_{\Delta\tau}(t)\,F_{T_a'}(t)\,\mathrm{d}t}. \tag{97}$$

Again using the properties $p_{T_a'}(t)=S'_{T_a'}(t)$ and $p_{\Delta\tau}(t)=S'_{\Delta\tau}(t)$ we get

$$\begin{aligned}\tilde{p}'_{T_a}(s)\Big|_{s\downarrow 0} &= \frac{\int_0^\infty t\left(S_{\Delta\tau}(t)\,S'_{T_a'}(t)+S_{T_a'}(t)\,S'_{\Delta\tau}(t)\right)\mathrm{d}t}{\int_0^\infty p_{\Delta\tau}(t)\,F_{T_a'}(t)\,\mathrm{d}t}\\ &= \frac{\int_0^\infty t\left(S_{\Delta\tau}(t)\,S_{T_a'}(t)\right)'\mathrm{d}t}{\int_0^\infty p_{\Delta\tau}(t)\,F_{T_a'}(t)\,\mathrm{d}t}\\ &= -\frac{\int_0^\infty S_{\Delta\tau}(t)\,S_{T_a'}(t)\,\mathrm{d}t}{\int_0^\infty p_{\Delta\tau}(t)\,F_{T_a'}(t)\,\mathrm{d}t},\end{aligned}$$

provided that the integral in the numerator exists. The MFPT $\langle T_a\rangle$ thus reads

$$\langle T_a\rangle=\frac{\int_0^\infty S_{\Delta\tau}(t)\,S_{T_a'}(t)\,\mathrm{d}t}{\int_0^\infty p_{\Delta\tau}(t)\,F_{T_a'}(t)\,\mathrm{d}t}. \tag{98}$$

If we consider a deterministic $\Delta\tau$ and let this quantity go to infinity we see that this result will in fact approach the moment $\langle T'_a \rangle$. Setting $p_{\Delta\tau}(t) = \delta(t-\tau)$ for some constant $\tau > 0$, we get

$$\langle T_a \rangle = \frac{\int_0^\tau S_{T'_a}(t)\,\mathrm{d}t}{\int_0^\infty \delta(t-\tau) F_{T'_a}(t)\,\mathrm{d}t} = \frac{\int_0^\tau S_{T'_a}(t)\,\mathrm{d}t}{F_{T'_a}(\tau)} \xrightarrow{\tau\to\infty} \int_0^\infty S_{T'_a}(t)\,\mathrm{d}t = \langle T'_a \rangle. \tag{99}$$

This also shows that for sharp resetting (deterministic, positive $\Delta\tau$) the mean will always be finite.

4.2. Complete resetting—examples

4.2.1. Poissonian resetting

Using expression (91) we find

$$\tilde{p}_{T_a}(s) = \frac{\tilde{p}_{T'_a}(s+r)}{1 - r\tilde{S}_{T'_a}(s+r)} = \frac{\tilde{p}_{T'_a}(s+r)}{1 - r\left(\frac{1}{s+r} - \frac{\tilde{p}_{T'_a}(s+r)}{s+r}\right)} = \frac{(s+r)\tilde{p}_{T'_a}(s+r)}{s + r p_{T'_a}(s+r)} \overset{r\downarrow 0}{\to} \tilde{p}_{T'_a}(s), \tag{100}$$

where we used the property of the Laplace transform of the survival probability, $\tilde{S}_{T'_a}(s) = (1 - \tilde{p}_{T'_a}(s))/s$. This confirms the convergence to the original FPT PDF in the absence of resetting ($r \downarrow 0$). Then the MFPT is equal to

$$\langle T_a \rangle = -\frac{\mathrm{d}t}{\mathrm{d}ts}\tilde{p}_{T_a}(s+r)\Big|_{s\downarrow 0} = \frac{\left(\tilde{p}_{T'_a}(r)\right)^{-1} - 1}{r}. \tag{101}$$

Setting $f(r) = (\tilde{p}_{T'_a}(r))^{-1}$ we aim at determining the optimal resetting rate r_o by minimising $\langle T_a \rangle$ as a function of r, i.e.

$$\langle T_a \rangle'(r) = \frac{rf'(r) - f(r) + 1}{r^2} = 0 \implies r_o f'(r_o) - f(r_o) - 1 = 0. \tag{102}$$

If it exists, solutions to this equation will be the optimal resetting rates for the first-passage problem.

4.2.2. Brownian motion

Setting $\tilde{p}_{T'_a}(s) = \exp(-a\sqrt{2s})$ we obtain $\langle T_a \rangle(r) = [\exp(a\sqrt{2r}) - 1]/r$, and the optimum resetting rate is a solution of the condition

$$a\sqrt{r_o} - \mathrm{e}^{-a\sqrt{2r_o}} = 1, \tag{103}$$

which is consistent with classical results [18].

4.2.3. SBM

For SBM we have [44]

$$p_{T'_a}(t) = \frac{a\alpha}{\sqrt{4\pi K_\alpha}} \exp\left(-\frac{a^2}{4K_\alpha t^\alpha}\right) t^{-1-\alpha/2}. \tag{104}$$

In Laplace space this PDF has the form

$$\tilde{p}_{T'_a}(s) = \frac{a\alpha}{\sqrt{4\pi K_\alpha}} \int_0^\infty t^{-1-\alpha/2} \exp\left(-\frac{a^2}{4K_\alpha t^\alpha} - st\right) \mathrm{d}t. \tag{105}$$

Using the definition of the Krätzel function we again rewrite expression (105) as

$$\tilde{p}_{T'_a}(s) = \frac{\sqrt{\pi}}{\alpha} Z_\alpha^{\frac{\alpha}{2}}\left(r\left[\frac{a^2}{4K_\alpha}\right]^{1/\alpha}\right). \tag{106}$$

After substituting this result into equation (101) we obtain the formula for the MFPT. It is shown in figure 9 as a function of α, while in figure 8 we show a favourable comparison with numerical simulations. In [44] a Laplace approximation of (105) was used. Maximising the function $t \mapsto -\frac{a^2}{4K_\alpha t^\alpha} - st$ leads to a maximum at $t_0 = (\alpha a^2/[4K_\alpha s])^{1/(\alpha+1)}$ and thus to the Laplace approximation of the form

$$\tilde{p}_{T'_a}(s) \approx \sqrt{\frac{2\alpha}{1+\alpha}} \exp\left(-s^{\frac{\alpha}{1+\alpha}}\left(\left(1+\frac{1}{\alpha}\right)\left(\frac{\alpha a^2}{4K_\alpha}\right)^{\frac{1}{1+\alpha}}\right)\right). \tag{107}$$

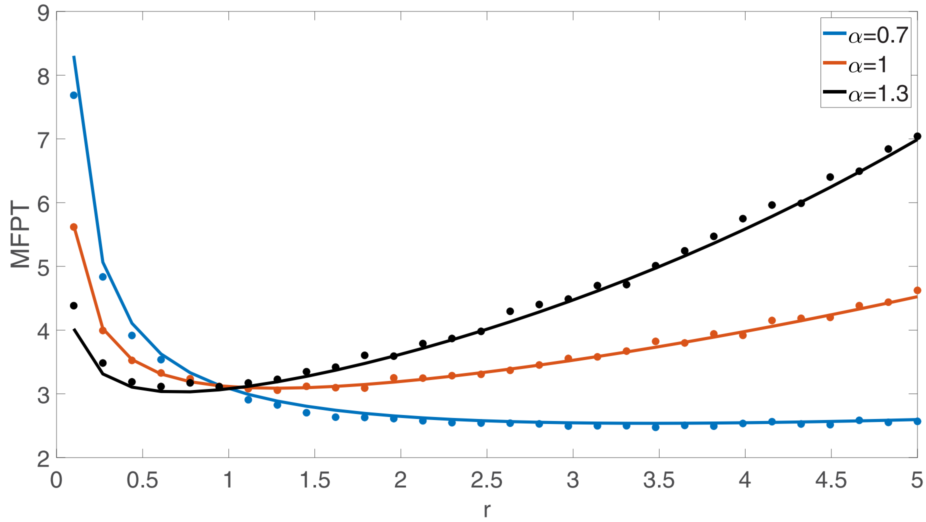

Figure 8. Comparison of the MFPT for different α for SBM under complete Poissonian resetting as a function of resetting rate. The lines represent the analytical result (106), the dots are results from Monte-Carlo simulations.

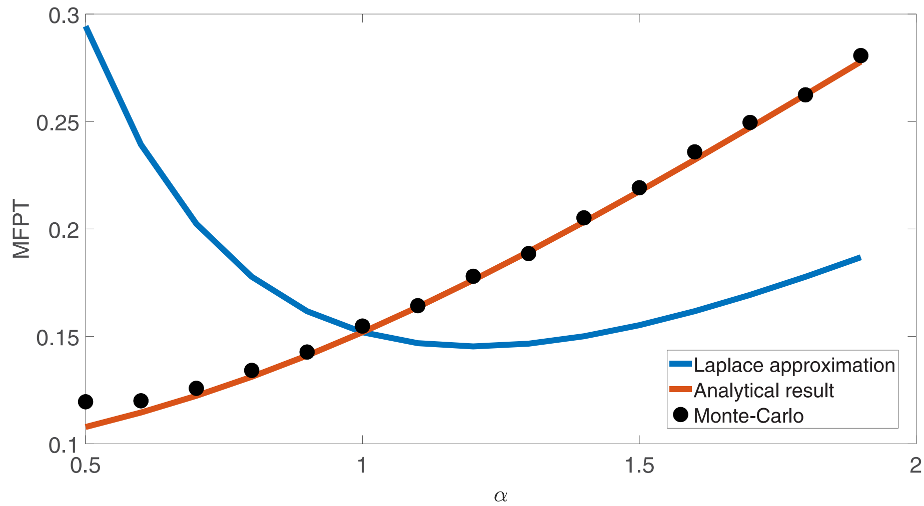

Figure 9. Comparison of the MFPT for SBM as a function of α obtained from the Laplace method (108) (blue line), with numerical evaluation of the Krätzel function (106) (red line) and with results from Monte-Carlo simulations (black dots, $N = 10^5$).

Substitution of this result into equation (101) yields

$$\langle T_a \rangle \approx \frac{1}{r}\left\{\sqrt{\frac{1+\alpha}{2\alpha}}\exp\left(r^{\frac{\alpha}{1+\alpha}}\left[\left(1+\frac{1}{\alpha}\right)\left(\frac{\alpha a^2}{4K_\alpha}\right)^{\frac{1}{1+\alpha}}\right]\right)-1\right\} \overset{\alpha\to 1}{\to} \frac{e^{a\sqrt{2r}}-1}{r}, \tag{108}$$

thus correctly reducing to the Brownian case. However, this Laplace approach is again burdened with a certain error, especially for smaller α values, as can be seen in figure 9. Moreover, in formula (108) the approximated PDF of T_a' lacks a proper normalisation. The explicit expression in terms of the Krätzel function therefore has a clear advantage.

4.2.4. Mixture-exponentially distributed resetting times

We now consider the important case of mixture-exponentially distributed waiting times. Due to the relative simplicity of the calculations for mixture-exponential distributions, this case can be used to approximate any $p_{\Delta\tau}$, see also [82]. This will allow us to calculate the FPTD by applying the so-called De Vylder approximation technique, which is well known in insurance mathematics [64]. It will also allow us to use results derived for mixture-exponential distributions to approximate results for other classes of distributions.

The general procedure is as follows: suppose that we want to approximate the FPTD or MFPT corresponding to some distribution of $\Delta\tau$, for which exact analytical results are unknown. Applying the De

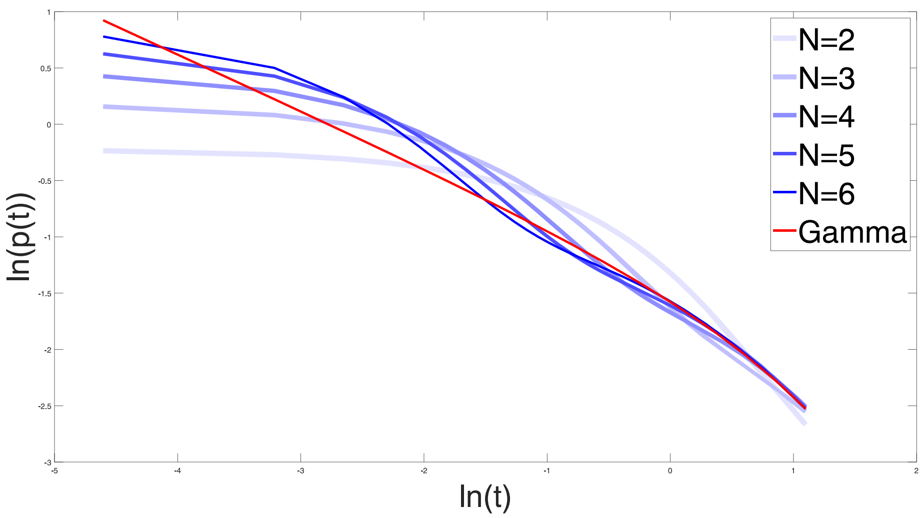

Figure 10. Approximating a $\Gamma(\frac{1}{2},5)$ distribution with a mixture-exponential distribution with $2N$ parameters using the method of moments described in the text. The method is time-consuming, yet the fit keeps improving.

Vylder approximation technique, we find the parameters of the corresponding mixture-exponential distribution, such that it robustly approximates the law of $\Delta\tau$. Next, using equation (91) we calculate the FPTD and MFPT corresponding to the resetting process with the above determined mixture-exponential waiting times.

Taking, for instance, Gamma-distributed waiting times $\Delta\tau \sim \Gamma(k,\vartheta)$, where k and ϑ are the shape and scale parameters, respectively, we approximate it using mixture-exponentially distributed waiting times $\Delta\tau^N$ with appropriately chosen parameters. More precisely, we choose $\Delta\tau^N$ to be the mixture of N exponential random variables with parameters $r_1, r_2, \ldots, r_N$ and weights $p_1, p_2, \ldots, p_N$. The PDF of $\Delta\tau$ is then given by

$$p_{\Delta\tau}(t;k,\vartheta) = \frac{1}{\Gamma(k)\vartheta^k} t^{k-1} \mathrm{e}^{-t/\vartheta}, \tag{109}$$

for $t \geqslant 0$. We assume for simplicity $k<1$, then the density of $\Delta\tau$ is monotone. We know that [84]

$$\langle(\Delta\tau)^n\rangle = \vartheta^n \frac{\Gamma(k+n)}{\Gamma(k)}, \tag{110}$$

and that

$$\begin{aligned}\langle(\Delta\tau^N)^n)\rangle &= \int_0^\infty t^n p_{\Delta\tau^N}(t)\mathrm{d}t = \sum_{i=1}^N p_i \int_0^\infty t^n p_{\Delta\tau^{N,i}}(t)\mathrm{d}t \\ &= \sum_{i=1}^N p_i \left\langle \left(\Delta\tau^{N,i}\right)^n \right\rangle = n! \sum_{i=1}^N \frac{p_i}{(r_i)^n},\end{aligned} \tag{111}$$

where we denoted by $\Delta\tau^{N,i} \sim \mathrm{Exp}(r_i)$ the ith random exponential component of the mixture-exponential distribution with rate r_i. Now we have to choose the parameters $r_1, r_2, \ldots, r_N$ and $p_1, p_2, \ldots, p_N$ in such a way that the PDF of $\Delta\tau^N$ will robustly approximate the PDF of $\Delta\tau$. This is done by solving an appropriate set of $2N$ Equations. The first equation is $\sum_{i=1}^N p_i = 1$. The remaining $2N-1$ Equations will be set such that the first $2N-1$ moments of both PDF are equal. We can see the approximation results for different N in figure 10, demonstrating that the approximation improves with increasing N. Other methods to find the parameters of $\Delta\tau^N$ can also be applied; for instance, one may minimise the so-called Lévy–Prokhorov metric [85] or the 1-Wasserstein metric [86] between CDFs of the distributions.

We thus have a tool to approximate different classes of PDFs in terms of the mixture-exponential distribution. We will now derive FPT results for these mixture-exponential distribution of waiting times, before using these results to approximate FPTs in more complicated settings. From equation (91) we obtain that

$$\tilde{p}_{T_a}(s) = \frac{\int_0^\infty p_{T_a'}(s+r)\,\mathrm{d}tF_R(r)}{1-\int_0^\infty rS_{T_a'}(s+r)\,\mathrm{d}tF_R(r)} = \frac{\mathbb{E}\left(p_{T_a'}(s+R)\right)}{1-\mathbb{E}\left(RS_{T_a'}(s+R)\right)}. \tag{112}$$

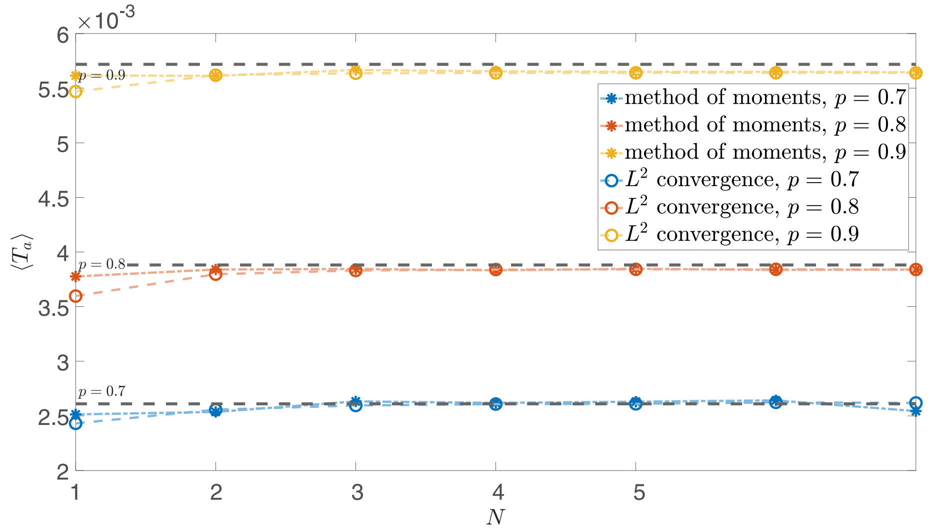

Figure 11. Comparison of the Monte-Carlo approximated MFPT (black dashed lines) for SBM under resetting with generalised gamma inter-resetting times and the mixture-exponential approximation with N components (coloured lines) obtained via the method of moments (stars) and minimising the L^2-distance between the PDFs (circles). We observe the convergence of the theoretical values to values slightly lower than those obtained from Monte-Carlo simulations; this is caused by the temporal discretisation in the simulations.

Choosing a discrete distribution for R as in (62), we have

$$\tilde{p}_{T_a}(s) = \frac{\sum_{i=1}^{n} p_i \tilde{p}_{T_a'}(s+r_i)}{1-\sum_{i=1}^{n} p_i r_i \tilde{S}_{T_a'}(s+r_i)} = \frac{\sum_{i=1}^{n} p_i \tilde{p}_{T_a'}(s+r_i)}{1-\sum_{i=1}^{n} p_i r_i \frac{1-\tilde{p}_{T_a'}(s+r_i)}{s+r_i}}$$

$$= \frac{\sum_{i=1}^{n} p_i \tilde{p}_{T_a'}(s+r_i)}{1-\sum_{i=1}^{n} \frac{p_i r_i}{s+r_i} + \sum_{i=1}^{n} \frac{p_i r_i \tilde{p}_{T_a'}(s+r_i)}{s+r_i}}. \tag{113}$$

Calculating the MFPT as before, we find

$$\langle T_a \rangle = \left(\sum_{i=1}^{n} \frac{p_i}{r_i} \left(1-\tilde{p}_{T_a'}(r_i)\right) \right) \Big/ \left(\sum_{i=1}^{n} p_i \tilde{p}_{T_a'}(r_i) \right). \tag{114}$$

We see that for $n=1$ this result correctly reduces to the Poissonian resetting case.

Going beyond the search for the optimal resetting rate for Poissonian resetting, we address the approximation of a PDF minimising the MFPT based on general mixture-exponential distribution. Consider a function $(\mathbf{r},\mathbf{p}) \mapsto \langle T_a \rangle(\mathbf{r},\mathbf{p})$, with the parameters $\mathbf{r} = (r_1,\ldots,r_n)$ and $\mathbf{p} = (p_1,\ldots,p_n)$ of a mixture-exponential distribution. We then define a linearly constrained multivariate nonlinear programming problem of finding $\mathbf{r}_o, \mathbf{p}_o$ that minimise the MFPT $\langle T_a \rangle(\mathbf{r},\mathbf{p})$ with the value $\langle T_a \rangle_o$. Note that we can also treat the $n \in \mathbb{N}_+$ parameters as a variable of the problem with optimal n_o, expecting $\langle T_a \rangle_o$ to decay with increasing n. The problem of choosing n in that case reduces to the problem of finding n_o which satisfies $\frac{\langle T_a \rangle_o(\mathbf{r},\mathbf{p},n_o+1)}{\langle T_a \rangle_o(\mathbf{r},\mathbf{p},n_o)} - 1 < \varepsilon$ for a given $\varepsilon > 0$. This is solvable by simple iteration of the aforementioned nonlinear programming problems for a constant n. This algorithm should return an optimal result under the mixed exponential regime.

4.2.5. SBM

We use the mixture-exponential approximation of the MFPT (114) to check the quality of the estimation for SBM with generalised gamma-distributed inter-resetting times. The PDF of $\Delta\tau$ is now

$$p_{\Delta\tau}(t;k,\vartheta,p) = \frac{p}{\Gamma\left(\frac{k}{p}\right)\vartheta^k} t^{k-1} \mathrm{e}^{-(t/\vartheta)^p} \tag{115}$$

Table 1. Relative errors of the mixture-exponential approximation technique for the case of SBM with generalised gamma-distributed inter-resetting times (115), obtained from the method of moments and minimising the L^2-distance between the corresponding PDFs. The mean of the inter-resetting time is different in each case for clarity. We observe the instability in the convergence of the method of moments as the error should decrease as $p \to 1$, when the PDF simplifies to the exponential case.

Method / p	0.7	0.8	0.9
Method of moments	0.13%	0.12%	0.46%
L^2 distance minimisation	0.34%	0.3%	0.24%

for $t \geqslant 0$, where we chose $k = 1$. This time we also use the minimisation of the L^2-error between the mixture-exponential and generalised gamma PDF as fitting technique. Selecting $\alpha = 2/3$, $a = 0.1$, $p = 0.7, 0.8, 9$ we obtain results closer to the Monte-Carlo simulations results as N increases, as seen in figure 11. The method of moments appears to be more unstable in this case, but the results still approach the correct values. The errors between Monte-Carlo simulations and theoretical values for $N = 8$ can be seen in table 1.

5. Conclusions

We introduced a series representation approach for stochastic processes with resetting in which the resetting dynamic is triggered by a renewal process. We considered the two scenarios of complete resetting, in which the memory of the parental process is erased, and incomplete resetting, which corresponds to a simple shifting of the position. Both definitions are equivalent for processes with stationary and independent increments. We calculated the PDF, the joint PDF at two points in time, and the autocorrelation function. We also studied the associated first-passage problems, for which we derived general formula for the PDF of the FPTs and the MFPT. The series representation offers a new and helpful method to obtain these quantities. Apart from the general results we obtained explicit results for exponentially (Poissonian resetting) and mixture-exponentially distributed inter-resetting times: the process PDF, autocorrelation function, FPTD and MFPT. The parental considered processes are Brownian motion and SBM. Finally, we devised a scheme for approximating the MFPT of a process with renewal resetting events by approximating its PDF using mixture-exponential distributions. We studied the quality of this approximation for SBM with generalised gamma-distributed inter-resetting times. All results were obtained using purely probabilistic methods.

We showed that the series representation technique offers an attractive and flexible alternative formulation for the analysis of SR. It should be of interest to expand the current analysis to different stochastic processes, such as fractional Brownian motion with long-ranged, power-law correlations of increments [87], continuous time random walks with different versions of waiting time and jump length PDFs [88], and others. The statistic of FPTs for processes with incomplete resetting has not been fully covered and needs further research. In figure 12 we show the comparison of the MFPTs for SBM as a function of resetting rate with exponential renewal times for both complete and incomplete resetting cases. We observe an interesting difference in the impact of the resetting type on the behaviour of the MFPT.

Overall, the series expansion of a stochastic process serves as a powerful tool in both theoretical studies and practical applications, offering efficiency, clarity, and analytical convenience. A striking example of such an approach is the Karhunen–Loève expansion of Brownian motion (see [89] and references therein), which can also be applied to Brownian motion with resetting, and is the subject of our current research. One of its primary benefits is the dimensionality reduction. This allows for an accurate approximation of the process using a finite number of components, which reduces computational demands and simplifies storage. Moreover it results in the spectral decomposition of the process with minimum representation entropy property. Another advantage is the simplification of mathematical and statistical analysis. It transforms the process into a series in which the random coefficients are uncorrelated. This diagonalisation of the covariance structure makes it easier to analyse and manipulate the process, particularly in applications such as prediction, estimation, Bayesian inference and filtering. The expansion provides insight into the structure of the process as well. The basis functions used in the expansion reflect dominant patterns or frequencies within the process, which can aid in understanding the underlying dynamics, detecting anomalies, or extracting features for further analysis. Finally, series expansions enhance mathematical tractability. When analysing systems governed by differential or integral equations, representing the random process in an appropriate basis often simplifies the equations, enabling analytical or semi-analytical solutions and facilitating stability and sensitivity analysis.

It should also be interesting to extend this framework to so-called partial stochastic resetting (PSR), in which the particle is not reset to its origin but to some value, a fixed or random fraction, in between the current state and the initial value. PSR was studied in mathematical [90, 91], financial and actuarial [92–96]

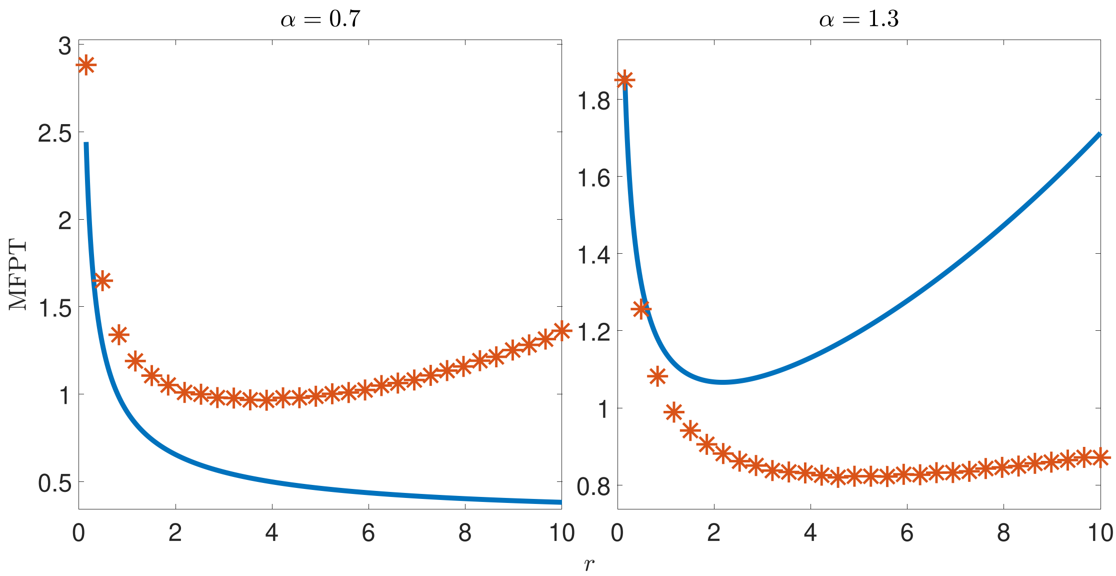

Figure 12. Comparison of the behaviour of the SBM-MFPT as function of the resetting rate for the cases of complete and incomplete Poissonian resetting from Monte-Carlo simulation. The blue lines are the theoretical results for the MFPT in the complete resetting case, the red stars are Monte-Carlo estimated MFPTs in the incomplete resetting case for $N = 10^5$ simulations.

literature, as well as in queueing theory [97]. Similar models are used in population dynamics [98–102]. PSR is also relevant for other observables, such as the amount of traffic over the internet, the size of a population, or the income of an insurance company. PSR can follow scenarios of independent or dependent resetting [103]. The case of dependent resetting, when the quantity cannot be negative, was analysed in [103–106], and the time-dependent solution was reported in [107].

We end with some remarks on the fact that our approach can be extended to various other processes. Let us denote

$$Y(t) = \sum_{i=0}^{\infty} F_i\left[\{X_j\}, N, \omega\right](t)\,\mathbf{1}_{N(t)=i} = F_{N(t)}\left[\{X_j\}, N, \omega\right](t), \tag{116}$$

where F_i are random operators acting on the trajectories of all X_j copies as well as on N. We see that the process Y can carry memory and 'look into the future' in the sense that F_i acts on the whole (global) trajectories of $N(t), X_0(t), X_1(t)\ldots$ for $t \geqslant 0$. This is a general representation that can be used for the definition of a wide class of processes, e.g.

(i) sign switching, $F = (-1)^{N(t)}X_0(t)$,
(ii) randomised exponential decay, $F_i = \mathrm{e}^{-\lambda(t-\tau_i)}X_0(t)$,
(iii) regime switching, $F_i = \sigma_i X_i(t-\tau_n) + \sum_{j=0}^{i-1}\sigma_j X_j(\tau_{j+1}-\tau_j)$,
(iv) run and tumble under resetting [108], $F_i = Y_i(X_{i-1})X_i(t-\tau_i)$, $Y_i(Z) = \mathrm{sgn}\,(Z(\tau_i-\tau_{i-1}))$ with probability η, $-\mathrm{sgn}\,(Z(\tau_i-\tau_{i-1}))$ with probability $1-\eta$, $Y_0 = 1$ a.s. $X_i(t) = v_0 t$.

This approach thus allows us to construct and analyse various stochastic processes. The usual methodology to study processes with resetting immediately turns to renewal equations [18, 44, 109]. There, one uses the descriptive definition of the process to derive equations for some finite-dimensional distribution. For instance, consider example (i), i.e. the sign switching process in which $N(t)$ is a Poisson process. Using this approach for the one-dimensional distributions we get the last-renewal equation

$$p_Y(x,t) = p_X(x,t)\,\mathrm{e}^{-rt} + r\mathrm{e}^{-rt}\int_0^t\int_{\mathbb{R}} p_Y(z,u)\,p_{X|X(0)=-z}(x,t-u)\,\mathrm{d}z\mathrm{d}u, \tag{117}$$

or, alternatively, the first-renewal equation

$$p_Y(x,t) = p_X(x,t)\,\mathrm{e}^{-rt} + r\int_0^t \mathrm{e}^{-ru}p_Y(-x,t-u)\,\mathrm{d}u. \tag{118}$$

In the last-renewal equation (117) the first term corresponds to the probability that there was no jump. The second term averages possible routes the process may undergo since the last reset from an arbitrary point z up to time t using the transition PDF p_X. The first-renewal equation (118) is indeed much simpler; while the first term is the same as in equation (117), the second term introduces a sign-flipping mechanic. Without the microscopic picture we could not even be sure if this probability corresponds to a stochastic process in the standard sense—or a generalised stochastic process without more context. The way shown here more directly reveals insights but lacks a certain rigour, and it does not allow a more general approach to solving other problems than the one stated previously—for instance, every equation for different finite-dimensional distributions has to be derived separately using different descriptions of the process. The series representation approach may have the same level of computational complexity, but it does not require any heuristic descriptions of the macroscopic properties of a process by considering the underlying probability flows. Meanwhile, it allows us to formally define a microscopic picture and analyse this object. Furthermore, by using it we can calculate properties of the process simply by definition. Our reasoning is that this approach has value due to automatisation of calculations.

Data availability statement

No new data were created or analysed in this study.

Acknowledgments

This research was partially supported by *Narodowe Centrum Nauki* Sonata Bis-9 Grant 2019/34/E/ST1/00360. Funding from the German Science Foundation (DFG, Grant numbers ME 1535/12-1 and ME 1535/22-1) is acknowledged, as well.

ORCID iDs

Kacper Taźbierski 0000-0002-2925-6013
Ralf Metzler 0000-0002-6013-7020
Marcin Magdziarz 0000-0002-2239-7155

References

[1] Smoluchowski M 1916 *Phys. Z.* **17** 585
[2] Gudowska-Nowak E, Lindenberg K and Metzler R 2017 *J. Phys. A* **50** 380301
[3] Bachelier L 1900 *Annal. scient. de l'E.N. S* **3** 21
[4] Lundberg F 1903 *Approximerad framställning av sannolikehetsfunktionen.terförsäkering av kollektivrisker* (Almqvist & Wiksell)
[5] Schrödinger E 1915 *Phys. Z.* **16** 289
[6] Redner S 2001 *A Guide to First Passage Processes* (Cambridge University Press)
[7] Metzler R, Oshanin G and Redner S (eds) 2014 *First-Passage Phenomena and Their Applications* (World Scientific)
[8] Grebenkov D, Metzler R and Oshanin G (eds) 2024 *Target Search Problems* (Springer)
[9] Coolidge J L 1909 *Ann. Math.* **10** 181
[10] Shlesinger M F 2021 *An Unbounded Experience in Random Walks With Applications* (World Scientific)
[11] Bénichou O, Chevalier C, Klafter J, Meyer B and Voituriez R 2010 *Nat. Chem.* **2** 472
[12] Bénichou O and Voituriez R 2014 *Phys. Rep.* **539** 225
[13] Godec A and Metzler R 2016 *Phys. Rev. X* **6** 041037
[14] Grebenkov D, Metzler R and Oshanin G 2018 *Commun. Chem.* **1** 96
[15] Grebenkov D, Metzler R and Oshanin G 2020 *New J. Phys.* **22** 103004
[16] Evans M R and Majumdar S N 2011 *Phys. Rev. Lett.* **106** 160601
[17] Evans M R and Majumdar S N 2011 *J. Phys. A* **44** 435001
[18] Evans M R, Majumdar S N and Schehr G 2020 *J. Phys. A* **53** 193001
[19] Perfetto G, Carollo F, Magoni M and Lesanovsky I 2021 *Phys. Rev. B* **104** L180302
[20] Besga B, Bovon A, Petrosyan A, Majumdar S N and Ciliberto S 2020 *Phys. Rev. Res.* **2** 032029(R)
[21] Pal A, Kundu A and Evans M R 2016 *J. Phys. A* **49** 225001
[22] Bhat U, De Bacco C and Redner S 2016 *J. Stat. Mech.* 083401
[23] Rotbart T, Reuveni S and Urbakh M 2015 *Phys. Rev. E* **92** 060101(R)
[24] Reuveni S 2016 *Phys. Rev. Lett.* **116** 170601
[25] Godrèche C and Luck J-M 2022 *J. Stat. Mech.* 063202
[26] Chechkin A V and Sokolov I M 2018 *Phys. Rev. Lett.* **121** 050601
[27] Sokolov I M 2023 *Phys. Rev. Lett.* **130** 067101
[28] Wald S and Böttcher L 2021 *Phys. Rev. E* **103** 012122
[29] Perfetto G, Carollo F and Lesanovsky I 2022 *SciPost Phys.* **13** 079
[30] Campos D, Bartumeus F, Méndez V and Espadaler X 2014 *J. R. Soc. Interface* **11** 20130859
[31] Kyriakidis E G 1994 *Stat. Prob. Lett.* **20** 239
[32] Montanari A and Zecchina R 2002 *Phys. Rev. Lett.* **88** 178701

[33] Blumer O, Reuveni S and Hirshberg B 2022 *J. Phys. Chem. Lett.* **13** 11230
[34] Viswanathan G M, da Luz M G E, Raposo E P and Stanley H E 2011 *The Physics of Foraging: an Introduction to Random Searches and Biological Encounters* (Cambridge University Press)
[35] Reuveni S, Urbakh M and Klafter J 2014 *Natl Acad. Sci. USA* **111** 4391
[36] Grange P 2021 *J. Phys. A* **54** 294001
[37] Durang X, Henkel M and Park H 2014 *J. Phys. A* **47** 045002
[38] Faisant F, Besga B, Petrosyan A, Ciliberto S and Majumdar S N 2021 *J. Stat. Mech.* 113203
[39] Altshuler A, Bonomo O L, Gorohovsky N, Marchini S, Rosen E, Tal-Friedman O, Reuveni S and Roichman Y 2024 *Phys. Rev. Res.* **6** 023255
[40] Tal-Friedman O, Pal A, Sekhon A, Reuveni S and Roichman Y 2020 *J. Phys. Chem. Lett.* **11** 7350
[41] Magdziarz M and Taźbierski K 2022 *Phys. Rev. E* **106** 014147
[42] Zhou T, Xu P and Deng W 2020 *Phys. Rev. Res.* **2** 013103
[43] Singh P and Pal A 2021 *Phys. Rev. E* **103** 052119
[44] Bodrova A S, Chechkin A V and Sokolov I M 2019 *Phys. Rev. E* **100** 012120
[45] Bodrova A, Chechkin A and Sokolov I 2019 *Phys. Rev. E* **100** 012119
[46] Olsen K S and Löwen H 2024 *J. Phys. A: Math. Theor.* 033210
[47] Wang W, Cherstvy A, Kantz H, Metzler R and Sokolov I 2021 *Phys. Rev. E* **104** 024105
[48] Sandev T, Domazetoski V, Kocarev L, Metzler R and Chechkin A 2022 *J. Phys. A* **55** 074003
[49] Bodrova A S and Sokolov I M 2020 *Phys. Rev. E* **101** 062117
[50] Shkilev V P and Sokolov I M 2022 *J. Phys. A* **55** 484003
[51] Vinod D, Cherstvy A, Wang W, Metzler R and Sokolov I 2022 *Phys. Rev. E* **105** L012106
[52] Vinod D, Cherstvy A, Metzler R and Sokolov I 2022 *Phys. Rev. E* **106** 034137
[53] Stojkoski V, Jolakoski P, Pal A, Sandev T, Kocarev L and Metzler R 2022 *Phil. Trans. R. Soc. A* **380** 20210157
[54] Ł K and Gudowska-Nowak E 2015 *Phys. Rev. E* **92** 052127
[55] Stanislavsky A and Weron A 2021 *Phys. Rev. E* **104** 014125
[56] Zelenkovski K, Sandev T, Metzler R, Kocarev L and Basnarkov L 2023 *Entropy* **25** 293
[57] Gupta S and Jayannavar A M 2022 *Front. Phys.* **10** 789097
[58] Abdoli I and Sharma A 2021 *Soft Matter* **17** 1307
[59] Petreska I, Pejov L, Sandev T, Kocarev L and Metzler R 2022 *Fract. Fract.* **6** 88
[60] Capała K, Dybiec B and Gudowska-Nowak E 2022 *Chaos* **32** 063129
[61] Sunil J C, Blythe R A, Evans M R, and Majumdar S N 2023 *J. Phys. A* **56** 395001
[62] Calvert G R and Evans M R 2021 *Eur. Phys. J. B* **94** 228
[63] Singh R K, Metzler R and Sandev T 2025 *Chaos* **35** 011103
[64] De Vylder F 1978 *Scand. Actuar. J.* **1978** 114–119
[65] Stojkoski V, Sandev T, Kocarev L and Pal A 2022 *J. Phys. A* **55** 104003
[66] Karatzas I and Shreve S 1991 *Brownian Motion and Stochastic Calculus, Graduate Texts in Mathematics (113)* (Springer)
[67] Lim S C and Muniandy S V 2002 *Phys. Rev. E* **66** 021114
[68] Jeon J- H, Chechkin A V and Metzler R 2014 *Phys. Chem. Chem. Phys.* **16** 15811
[69] Ibe O C 2013 *Markov Processes for Stochastic Modeling* 2nd edn (Elsevier)
[70] Gradshteyn I S, Ryzhik I M, Zwillinger D and Moll V 2015 *Table of Integrals, Series and Products* (Academic)
[71] Mathai A M, Saxena R K and Haubold H J 2010 *The H-Function* (Springer)
[72] Kilbas A, Rodríguez-Germá L, Saigo M, Saxena R and Trujillo J J 2010 *Comput. Math. Appl.* **59** 1790–800
[73] Jovanović A P *et al* 2014 *Eur. Phys. J. Appl. Phys.* **67** 20801
[74] Abas N, Daud Z M and Yusof F 2014 *Theor. Appl. Climatol.* **118** 597
[75] Okada M, Yamanishi K, Masuda N and Soc R 2020 *Open Sci.* **7** 191643
[76] Siegle P, Goychuk I and Hänggi P 2011 *Europhys. Lett.* **93** 20002
[77] Koshak W J 2011 *J. Atmosph. Ocean. Technol.* **28** 475
[78] Shazwani N, Norzaida A and Syafrina A H 2018 *Int. J. Eng. Tech.* **7** 1412
[79] Cai N and Kou S G 2011 *Manage. Sci.* **57** 2067
[80] Wilk G and Włodarczyk Z 2002 *Chaos Solitons Fractals* **13** 581
[81] Bartlett M S, Daly E, McDonnell J J, Parolari A J and Porporato A 2015 *Proc. R. Soc. A* **471** 20150389
[82] Harris C M 1985 *Comp. Oper. Res.* **12** 285
[83] Rudin W 1984 *Real and Complex Analysis* (McGraw Hill)
[84] Papoulis A 1984 *Probability, Random Variables and Stochastic Processes* (McGraw Hill)
[85] Billingsley P 1999 Convergence of Probability Measures *(Wiley Series in Probability and Statistics)* (Wiley)
[86] Villani C 2009 *Optimal Transport: Old and New* (Springer)
[87] Mandelbrot B B and van Ness J W 1968 *SIAM Rev.* **10** 422
[88] Klafter J, Blumen A and Shlesinger M F 1987 *Phys. Rev. A* **35** 3081
[89] Wang L 2008 *Karhunen-Loeve Expansions and Their Applications* (London School of Economics)
[90] Dumas V, Guillemin F and Robert P 2002 *Adv. Appl. Probab.* **34** 85
[91] Lopker A and Stadje W 2011 *J. Appl. Probab.* **48** 295
[92] Asmussen S and Albrecher H 2010 *Ruin Probabilities* (World Scientific)
[93] Marciniak E and Palmowski Z 2016 *J. Optim. Theor. Appl.* **168** 723
[94] Hofstad R , Kapodistria S, Palmowski Z and Shneer S 2023 *J. Appl. Probab.* **60** 85
[95] Boxma O, Perry D, Stadje W and Zacks S 2006 *Adv. Appl. Probab.* **38** 221
[96] Boxma O, Perry D and Stadje W 2022 *Math. Meth. Methods Oper.* **96** 233
[97] van Leeuwaarden J S H and Ott T J 2009 *Queu. Syst.* **63** 459
[98] Hanson F B and Tuckwell H C 1981 *Theor. Popul. Biol.* **19** 1–18
[99] Gripenberg G 1983 *J. Math. Biol.* **17** 371
[100] Pakes A G 1987 *J. Math. Biol.* **25** 307
[101] Brockwell P J, Gani J and Resnick S I 1982 *Adv. Appl. Probab.* **14** 709

[102] Artalejo J R, Economou A and Lopez-Herrero M J 2006 *Math. Biosci. Eng.* **4** 573
[103] Dahlenburg M, Chechkin A, Schumer R and Metzler R 2021 *Phys. Rev. E* **103** 052123
[104] Pierce J K arXiv:2204.07215
[105] Toledo-Marin J Q and Boyer D 2023 *Phys. A* **625** 129027
[106] Tal-Friedman O, Roichman Y and Reuveni S 2022 *Phys. Rev. E* **106** 054116
[107] Di Bello C, Chechkin A, Hartmann A K, Palmowski Z and Metzler R 2023 *New J. Phys.* **25** 082002
[108] Evans M R and Majumdar S N 2018 *J. Phys. A* **51** 475003
[109] Majumdar S N and Oshanin G 2018 *J. Phys. A* **51** 435001